

Asset Pricing with General Transaction Costs: Theory and Numerics*

Lukas Gonon[†] Johannes Muhle-Karbe[‡] Xiaofei Shi[§]

June 6, 2019

Abstract

We study risk-sharing equilibria with general convex costs on the agents' trading rates. For an infinite-horizon model with linear state dynamics and exogenous volatilities, the equilibrium returns mean-revert around their frictionless counterparts – the deviation has Ornstein-Uhlenbeck dynamics for quadratic costs whereas it follows a doubly-reflected Brownian motion if costs are proportional. More general models with arbitrary state dynamics and endogenous volatilities lead to multidimensional systems of nonlinear, fully-coupled forward-backward SDEs. These fall outside the scope of known wellposedness results, but can be solved numerically using the simulation-based deep-learning approach of [28]. In a calibration to time series of returns, bid-ask spreads, and trading volume, transaction costs substantially affect equilibrium asset prices. In contrast, the effects of different cost specifications are rather similar, justifying the use of quadratic costs as a proxy for other less tractable specifications.

Mathematics Subject Classification: (2010) 91G10, 91G80, 60H10.

JEL Classification: C68, D52, G11, G12.

Keywords: Radner equilibrium, transaction costs, forward–backward SDEs, deep learning

1 Introduction

The interplay between *liquidity* and *asset prices* has been studied extensively in the empirical literature, cf., e.g., [5] and the references therein for an overview. The analysis of theoretical models consistent with the main stylized facts established in these studies is challenging, however, since both models with limited liquidity and equilibrium asset pricing models are notoriously intractable on their own right. These difficulties are of course only compounded for models where equilibrium asset prices are determined endogenously in the presence of trading frictions.

Accordingly, tractable models often focus on settings where asset prices [47, 38, 49] or trading volume [46] are deterministic. Models where asset prices and trading volume both fluctuate randomly have recently been analyzed by focusing on quadratic costs on the agents' trading

*We thank Bruno Bouchard, Agostino Capponi, and Robert Pego for fruitful discussions.

[†]University of St. Gallen, Faculty of Mathematics and Statistics, Bodanstrasse 6, 9000 St.Gallen, Switzerland, email lukas.gonon@unisg.ch.

[‡]Imperial College London, Department of Mathematics, London, SW7 1NE, UK, email j.muhle-karbe@imperial.ac.uk. Research supported by the CFM-Imperial Institute of Quantitative Finance.

[§]Carnegie Mellon University, Department of Mathematical Sciences, 5000 Forbes Avenue, Pittsburgh, PA 15213, USA, xiaofeish@andrew.cmu.edu.

rates [22, 43, 9, 29]. The analysis of these models crucially exploits the linearity of the corresponding first-order conditions, thereby naturally raising the question how delicately the qualitative and quantitative predictions depend on the specific choice of the trading costs. Typical examples are linear transaction taxes or empirical estimates of actual trading costs that typically correspond to a power of the order flow of around $3/2$ [37, 4].

The present study addresses this challenge by studying risk-sharing equilibria with *general* convex costs levied on the agents' trading rates. This nests quadratic costs as one special case, but also covers proportional costs as another limiting case. We show that in an infinite-horizon model with linear state dynamics and exogenous price volatility, the corresponding equilibrium returns can be characterized explicitly up to the solution of a single nonlinear ODE. The latter determines the mean-reverting fluctuations of the frictional equilibrium returns around their frictionless counterparts. If costs are quadratic, this "liquidity premium" is an Ornstein-Uhlenbeck process similarly as in [22, 9, 29]; for proportional costs it turns out to be a doubly-reflected Brownian motion.

To assess the quantitative differences between the respective equilibrium returns, we calibrate our model to market data. This is challenging, since agents' preferences and endowments are not directly observable. However, we show that this difficulty can be overcome as follows. We first pin down some of the parameters by calibrating the frictionless model to a time series of prices. Then, we fit the additional parameters of our model with proportional transaction costs to bid-ask spreads and trading volume data, by exploiting that the average turnover rate in the model can be computed in closed form. To obtain comparable results for other forms of trading costs, we in turn match the corresponding trading volumes and stationary variances of the liquidity premium.

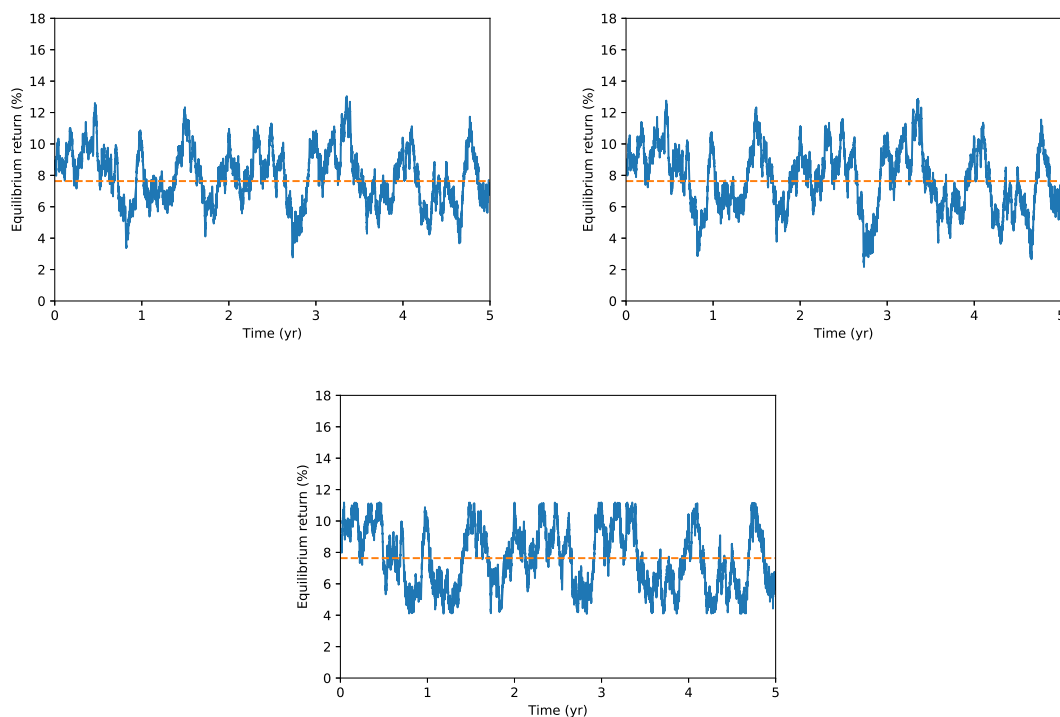


Figure 1: Simulated frictional equilibrium returns with calibrated parameters for quadratic trading costs (left upper panel), costs proportional to the $3/2$ -th power of the agents' trading rates (right upper panel), and proportional trading costs (lower panel). The corresponding (annual) frictionless equilibrium return is constant and equal to 7.64% here.

As shown in Figure 1, realistic trading costs lead to substantial fluctuations around the constant frictionless expected returns if agents' trading targets are calibrated to match the large trading volume observed empirically. In contrast, the differences between the results for proportional, quadratic, and intermediate costs are rather small if the magnitude of these costs is matched appropriately.

Trading volume is a nonlinear function of the equilibrium returns in our model, and this transformation magnifies the differences between different cost specifications. Indeed, for quadratic costs, volume follows the absolute value of an Ornstein-Uhlenbeck process, whereas subquadratic costs skew volume towards either zero or infinite rates as observed in the limiting case of proportional costs. As illustrated in Figure 2, the simulated order flow corresponding to the calibrated model with costs proportional to a power $3/2$ (in line with direct empirical estimates as in [37, 4]) rather than 2 of the order flow therefore comes closer to matching the substantial skewness and heavy tails observed in real data.

Nevertheless, the broad properties of both models are rather similar. Accordingly, our results suggest that quadratic costs on the trading volume can indeed serve as a valuable proxy for other, less tractable, trading cost specifications.

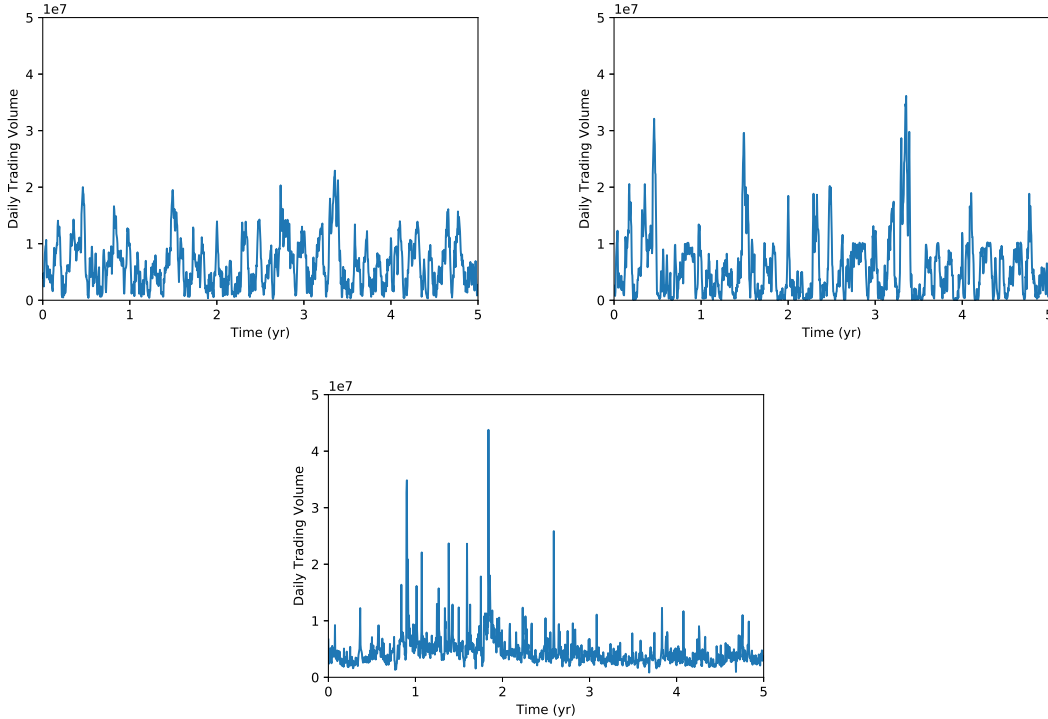


Figure 2: Trading volume for empirical time series (lower panel) and simulations with calibrated parameters for quadratic trading costs (left upper panel) and costs proportional to the $3/2$ -th power of the agents' trading rates (right upper panel).

To analyze whether this remains true in more general settings, we extend our baseline model to more general state dynamics and endogenous volatilities determined by matching an exogenous terminal dividend. This allows to study how changes in market liquidity feed back into price fluctuations, e.g., how volatility is affected by the introduction of a financial transaction tax.

Such more general models lead to fully-coupled systems of nonlinear forward-backward stochastic differential equations. To wit, the optimal positions evolve forward from the agents' initial

allocations. In contrast, the initial optimal trading rates need to be determined as part of the solution, taking into account that trading stops at the terminal time. Likewise, the stock dynamics also need to be derived from the terminal dividend. For quadratic trading costs, wellposedness of this multidimensional and fully coupled system has recently been established by [29] for agents with sufficiently similar risk aversions. If trading costs are not quadratic, wellposedness of the system is a challenging open problem, and simplifications to systems of coupled Riccati equations as in [29] are not possible even with linear state dynamics.

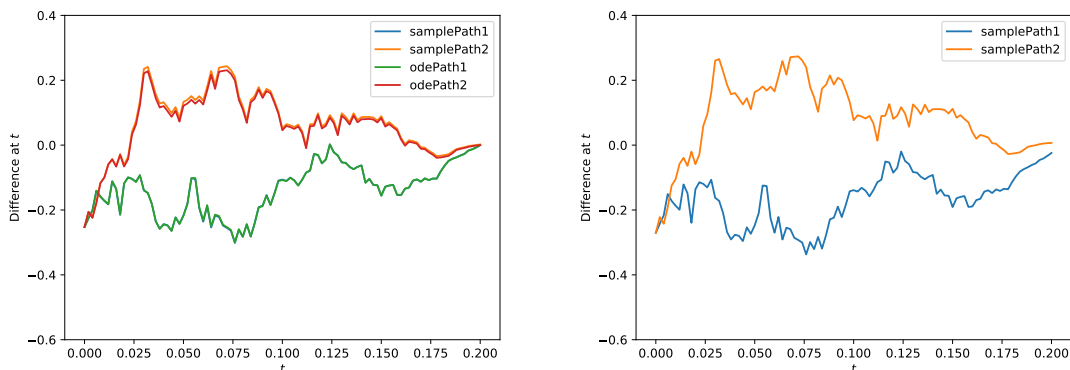


Figure 3: Difference between simulated frictional and frictionless equilibrium prices with calibrated parameters for quadratic costs (left panel) and 3/2-costs (right panel).

However, we demonstrate that, the system can be solved numerically by adapting the simulation-based deep learning approach of [28] if the time horizon is not too long. Here, the idea is to use a deep neural network to parametrize the “decoupling field” that describes the backward components as a function of the forward variables. For each choice of the decoupling field, the corresponding forward dynamics of the system can in turn be simulated by a standard Euler scheme, so that it remains to keep updating the initial guess for the decoupling field using stochastic gradient descent until the simulation matches the terminal condition of the equation sufficiently well.

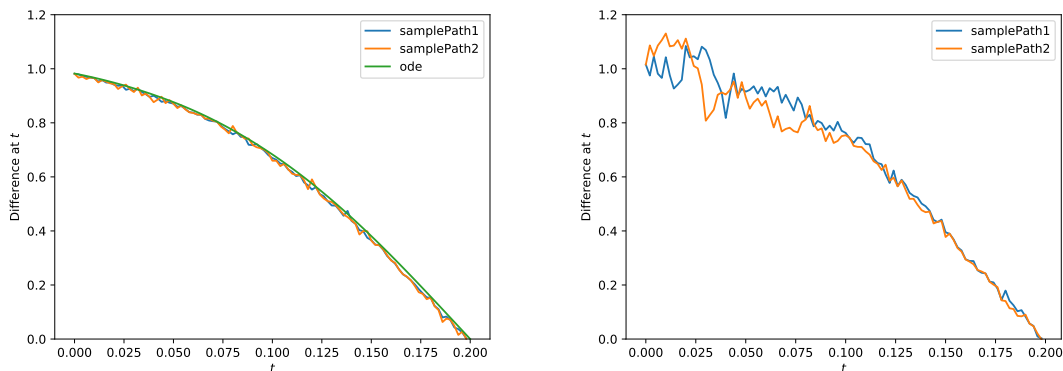


Figure 4: Difference between simulated frictional and frictionless equilibrium volatilities with calibrated parameters for quadratic costs (left panel) and 3/2-costs (right panel).

We verify that our algorithm produces accurate results by comparing it to the Riccati system that describes the equilibrium in a benchmark example with quadratic costs and linear state

dynamics in [29]. With minor adjustments, the same algorithm is also able to deal with other trading cost specifications. This is illustrated in Figure 3, where we plot the differences between frictional and frictionless equilibrium prices for quadratic costs and costs equal to the 3/2-th power of the agents' trading rates as in [1, 4]. Again, the precise choice of the trading cost only leads to small effects, even though the equilibrium volatility adjustment is deterministic for quadratic costs (as shown analytically in [29] and confirmed numerically in the left panel of Figure 4), but a mean-reverting stochastic process for 3/2-costs, see the right panel of Figure 4.

The remainder of this article is organized as follows. Section 2 introduces our frictionless baseline model and derives the corresponding equilibrium returns. In Section 3 this model and the equilibrium results are extended to general smooth convex costs on the agents' trading rates. The limiting case of proportional transaction costs is treated separately in Section 4. Both models are calibrated to time series data in Section 5. Equilibrium prices in more general models with arbitrary state dynamics and endogenous volatilities are linked to nonlinear FBSDEs in Section 6 and solved numerically in Section 7. For better readability, all proofs are collected in Section 8 as well as Appendices A and B.

Notation Fix a filtered probability space $(\Omega, \mathcal{F}, (\mathcal{F}_t)_{t \geq 0}, \mathbb{P})$ supporting a standard Brownian motion $(W_t)_{t \geq 0}$ and denote by \mathcal{L}^p the adapted processes $(X_t)_{t \geq 0}$ that satisfy $\mathbb{E}[\int_0^T |X_t|^p dt] < \infty$ for all $T > 0$.

2 Frictionless Baseline Model

2.1 Risk-Sharing Economy

We consider two agents indexed by $n = 1, 2$ that receive (cumulative) random endowments

$$d\zeta_t^n = \beta_t^n dW_t, \quad \text{where } \beta_t^n = \beta^n W_t, \quad \beta^n \in \mathbb{R}.$$

To hedge against the fluctuations of their endowments, the agents trade a safe and a risky asset. The price of the safe asset is exogenous and normalized to one. The price of the risky asset follows

$$dS_t = \mu_t dt + \sigma dW_t.$$

Here, the constant volatility σ is given exogenously, whereas the expected returns process $\mu \in \mathcal{L}^2$ is to be determined endogenously by matching the agents' demand to the fixed supply $s \in \mathbb{R}$ of the risky asset; see [46, 51, 16, 33, 22, 50, 9] for related equilibrium models where the volatility is a free parameter. Models where the volatility is determined endogenously are discussed in Section 6.

2.2 Frictionless Optimization and Equilibrium

As a reference point, we first consider the frictionless version of the model. Starting from fixed initial positions that clear the market, $\varphi_{0-}^1 + \varphi_{0-}^2 = s$, the agents choose their positions $\varphi \in \mathcal{L}^2$ in the risky asset to maximize one-period expected returns penalized for the corresponding variances. Without transaction costs, the continuous-time version of this criterion is

$$\bar{J}_T^n(\varphi) = \mathbb{E} \left[\int_0^T (\varphi_t dS_t + d\zeta_t^n) - \frac{\gamma^n}{2} d\langle \int_0^\cdot \varphi_u dS_u + \zeta^n \rangle_t \right] = \mathbb{E} \left[\int_0^T \left(\varphi_t \mu_t - \frac{\gamma^n}{2} (\sigma \varphi_t + \beta_t^n)^2 \right) dt \right]. \quad (2.1)$$

Put differently, agents trade off expected returns against the tracking error relative to the exogenous target position $-\beta^n/\sigma$ as in [17, 43]. The optimal strategy for (2.1) is readily determined by pointwise optimization as

$$\varphi_t^n = \frac{\mu_t}{\gamma^n \sigma^2} - \frac{\beta_t^n}{\sigma}, \quad t \in [0, T].$$

The equilibrium return is in turn pinned down by matching the agents' total demand $\varphi_t^1 + \varphi_t^2$ to the supply s of the risky asset at all times $t \in [0, T]$:

$$\bar{\mu}_t = \bar{\gamma} [s\sigma^2 + \sigma(\beta_t^1 + \beta_t^2)], \quad t \in [0, T], \quad \text{where } \bar{\gamma} = \frac{\gamma^1 \gamma^2}{\gamma^1 + \gamma^2}. \quad (2.2)$$

The agents' optimal trading strategies corresponding to this frictionless equilibrium return are

$$\bar{\varphi}_t^1 = \frac{s\gamma^2}{\gamma^1 + \gamma^2} + \frac{\gamma^2 \beta_t^2 - \gamma^1 \beta_t^1}{(\gamma^1 + \gamma^2)\sigma} \quad \bar{\varphi}_t^2 = s - \bar{\varphi}_t^1, \quad t \in [0, T].$$

Note that the frictionless equilibrium return and the corresponding optimal trading strategies are independent of the time horizon T . In particular, the frictionless optimizers also maximize the long-run average performance \bar{J}_T^n/T as $T \rightarrow \infty$, in that

$$\limsup_{T \rightarrow \infty} \frac{1}{T} [\bar{J}_T^n(\psi) - \bar{J}_T^n(\varphi)] \leq 0, \quad \text{for all competing admissible strategies } \psi.$$

With transaction costs – where the optimizers are no longer independent of the planning horizon – we will directly solve the long-run version of (2.1), see Definitions 3.2 and 4.1 below.

3 Equilibrium with Costs on the Trading Rate

3.1 Costs and Strategies

We now take into account transaction costs. A popular class of models originating from the optimal execution literature [2, 1] focuses on absolutely continuous trading strategies,

$$\varphi_t = \varphi_{0-}^n + \int_0^t \dot{\varphi}_u du, \quad t \geq 0,$$

and penalizes the trading rate $\dot{\varphi}_t = d\varphi_t/dt$ with an *instantaneous trading cost* $G(\dot{\varphi}_t)$. Portfolio choice problems for the most tractable specification $G(x) = \lambda x^2/2$, $\lambda > 0$ are analyzed in single-agent models by [22, 3, 42, 26]; equilibrium returns are determined in [22, 43, 9]. In [27, 14, 8], single-agent models are solved for the more general power costs $G(x) = \lambda|x|^q/q$, $q \in (1, 2]$ proposed by [1]. Below, we will determine equilibrium returns for general smooth convex cost functions G as studied in the duality theory of [25]:

Assumption 3.1. (i) *The trading cost $G : \mathbb{R} \rightarrow \mathbb{R}_+$ is convex, symmetric, and strictly increasing on $[0, \infty)$, differentiable on $[0, \infty)$, and satisfies $G(0) = 0$;*

(ii) *The derivative G' is also strictly increasing and differentiable on $(0, \infty)$ with $G'(0) = 0$;*

(iii) *There exist constants $C > 0$, $k \geq 2$ and $x_0 > 0$ such that*

$$|(G')^{-1}(x)| \leq C(1 + |x|^{k-1}) \text{ for all } x \in \mathbb{R}, \quad ((G')^{-1})'(x) \geq \frac{1}{C} \text{ for all } |x| > x_0.$$

One readily verifies that the power functions $G(x) = \lambda|x|^q/q$, $q \in (1, 2]$ proposed in [1] satisfy all of these requirements. So do linear combinations of these power functions, for example.

With transaction costs, the analogue of the frictionless mean-variance goal functional (2.1) is

$$J_T^n(\dot{\varphi}) = \mathbb{E} \left[\int_0^T \left(\varphi_t \mu_t - \frac{\gamma^n}{2} (\sigma \varphi_t + \beta_t^n)^2 - G(\dot{\varphi}_t) \right) dt \right]. \quad (3.1)$$

Unlike its frictionless counterpart, this optimization problem is no longer “myopic”, since the current position influences future choices in the presence of transaction costs, and since optimal strategies naturally depend on a finite time horizon T here. To simplify the analysis below, we therefore focus on the ergodic limit of (3.1), where the goal is to maximize the long-run average performance $J_T^n(\dot{\varphi})/T$ as $T \rightarrow \infty$. This criterion has a long history in single-agent problems with transaction costs, cf. [19, 45, 18, 23, 26]. Here, we show that it also allows to make the equilibrium analysis of general trading costs tractable. Throughout, we focus on *admissible* strategies

$$\varphi_t = \varphi_{0-}^n + \int_0^t \dot{\varphi}_u du, \quad t \geq 0$$

that satisfy the integrability conditions

$$\mathbb{E} \left[\int_0^T G(\dot{\varphi}_t) dt \right] < \infty, \quad \mathbb{E} \left[\int_0^T \varphi_t^2 dt \right] < \infty, \quad (3.2)$$

as well as the transversality condition

$$\lim_{T \rightarrow \infty} \frac{1}{T^2} \mathbb{E}[\varphi_T^2] = 0. \quad (3.3)$$

3.2 Equilibrium

Definition 3.2. $\mu \in \mathcal{L}^2$ is a (long-run) equilibrium return if there exist admissible trading rates $\dot{\varphi}^1, \dot{\varphi}^2$ for agents 1 and 2 such that:

(Market Clearing) The total demand $\varphi^1 + \varphi^2$ matches the supply s of the risky asset at all times;

(Individual Optimality) The trading rate $\dot{\varphi}^n$ is optimal for the long-run version of agent n 's control problem (3.1) in that,

$$\limsup_{T \rightarrow \infty} \frac{1}{T} \left[J_T^n(\dot{\psi}) - J_T^n(\dot{\varphi}^n) \right] \leq 0, \quad \text{for all competing admissible trading rates } \dot{\psi}. \quad (3.4)$$

The construction of the equilibrium return is based on the solution of a nonlinear ODE. For single-agent models with instantaneous trading costs of power form, a corresponding equation has been introduced and studied by [27].¹ In Appendix A, we show that their existence and uniqueness proof can be extended to general cost functions satisfying Assumption 3.1.

¹Indeed, if $G(x) = \lambda|x|^q/q$, $q \in (1, 2]$, set $\delta^2 = \gamma\sigma^2$, $2^{q-1}q = \delta^{2q-2}\lambda$ as well as $q = \alpha + 1$ in (3.5). Then, differentiating the first-order ODE (17) in [27, Theorem 6] leads to the second-order ODE (3.5). The same link to a first-order equation is exploited in our existence proof in Appendix A.

Lemma 3.3. *Suppose the instantaneous trading cost G satisfies Assumption 3.1 and define*

$$\gamma = \frac{\gamma^1 + \gamma^2}{2}, \quad \delta = \frac{\gamma^1 \beta^1 - \gamma^2 \beta^2}{(\gamma^1 + \gamma^2)\sigma}.$$

Then the ordinary differential equation

$$\frac{1}{2}\delta^2 g''(x) + g'(x)(G')^{-1}(g(x)) = \gamma\sigma^2 x \quad (3.5)$$

has a unique solution g on \mathbb{R} such that $xg(x) \leq 0$ for all $x \in \mathbb{R}$. Moreover, g satisfies

$$\lim_{x \rightarrow -\infty} \frac{g(x)}{(G^*)^{-1}(\frac{\gamma\sigma^2}{2}x^2)} = 1, \quad \lim_{x \rightarrow +\infty} \frac{g(x)}{(G^*)^{-1}(\frac{\gamma\sigma^2}{2}x^2)} = -1, \quad (3.6)$$

where G^ is the Legendre transform of G .*

Proof. See Appendix A. □

With the function g from Lemma 3.3, we can now define the state variable that will drive both the expected returns and optimal trading rates in equilibrium.

Lemma 3.4. *Let g be the solution of the ODE (3.5) from Lemma 3.3. There exists a unique strong solution of the SDE*

$$dX_t = (G')^{-1}[g(X_t)]dt + \delta dW_t, \quad t \geq 0, \quad X_0 = \varphi_{0-}^1 - \frac{s\gamma^2}{\gamma^1 + \gamma^2}. \quad (3.7)$$

Proof. This follows from results of [48], see Section 8.1. □

Remark 3.5. If the instantaneous trading cost is quadratic, $G(x) = \lambda x^2/2$, then $(G')^{-1}[x] = x/\lambda$, and the solution of (3.5) from Lemma 3.3 is $g(x) = -\sqrt{\gamma\lambda}\sigma x$. Accordingly, the dynamics (3.7) simplify to

$$dX_t = -\sqrt{\frac{\gamma}{\lambda}}\sigma X_t dt + \delta dW_t, \quad t \geq 0, \quad X_0 = \varphi_{0-}^1 - \frac{s\gamma^2}{\gamma^1 + \gamma^2}.$$

Whence, X is an Ornstein-Uhlenbeck process in this case. In general, the drift rate in (3.7) describes the nonlinear attraction of the process X towards its average level zero, where $xg(x) \leq 0$ ensures that the process is indeed mean reverting.

We now present our first main result. It identifies the equilibrium return for general smooth, convex cost functions.

Theorem 3.6. *With the solution $(X_t)_{t \geq 0}$ of (3.7), define*

$$\mu_t = \bar{\gamma} [s\sigma^2 + \sigma(\beta_t^1 + \beta_t^2)] + \frac{(\gamma^1 - \gamma^2)\sigma^2}{2} X_t, \quad t \geq 0. \quad (3.8)$$

Then, the trading rates

$$\varphi_t^1 = (G')^{-1}[g(X_t)], \quad \varphi_t^2 = -(G')^{-1}[g(X_t)], \quad t \geq 0 \quad (3.9)$$

clear the corresponding market and are individually optimal in the long run. Therefore, $(\mu_t)_{t \geq 0}$ is an equilibrium return.

Proof. See Section 8.1. □

The first term in (3.8) is the frictionless equilibrium return from (2.2). Accordingly, the second term describes how the equilibrium return changes due to transaction costs. Evidently, if both agents have the same risk aversion, then the adjustment is zero like for the quadratic costs studied by [9]. In this case, both agents are adversely affected by the transaction costs, but the market still clears at the frictionless equilibrium price.

For heterogenous agents, there is a nontrivial liquidity premium depending on the current demand imbalance. Indeed, in equilibrium, the state dynamics dX_t also describe the evolution of the deviation between agent 1's actual position and its frictionless counterpart,

$$dX_t = (G')^{-1}[g(X_t)]dt + \delta dW_t = (G')^{-1}[g(X_t)]dt + \frac{\gamma^1\beta^1 - \gamma^2\beta^2}{(\gamma^1 + \gamma^2)\sigma}dW_t = d(\varphi_t^1 - \bar{\varphi}_t^1).$$

By market clearing, the sign is reversed for agent 2. Accordingly, the liquidity premium is positive if the more risk averse agent wants to sell and negative if the more risk averse agent wants to buy to move closer to the corresponding frictionless allocation. In each case, the return adjustment ensures market clearing by offsetting the more risk averse agent's stronger motive to trade.

For quadratic costs, we recover the Ornstein-Uhlenbeck returns from [9, Corollary 5.5]. For general convex trading costs, these are replaced by processes with nonlinear mean-reversion speeds.

4 Equilibrium with Proportional Costs

One important cost specification is not covered by Assumption 3.1: proportional transaction costs. These arise as the limit $p \rightarrow 1$ in the model of [1]. Rather than studying the (singular) limiting behaviour of the corresponding optimal strategies as in [27], we instead show that the equilibrium with proportional costs can be constructed directly using singular rather than regular stochastic control.

Since proportional costs only penalize trade size but not speed, risky positions are naturally described by general finite-variation processes in this case or, equivalently, by their Jordan-Hahn decompositions into minimal increasing processes – the cumulative numbers of shares purchased and sold:

$$\varphi_t = \varphi_{0-}^n + \varphi_t^\uparrow - \varphi_t^\downarrow.$$

As in [31, 41, 18, 40] we assume for simplicity that the (cumulative) costs $\lambda(\varphi_T^\uparrow + \varphi_T^\downarrow)$, $\lambda > 0$, are proportional to the number of shares traded (rather than the monetary amount transacted). Agent n 's goal functional in turn becomes

$$J_T^n(\varphi) = \mathbb{E} \left[\int_0^T \left(\varphi_t \mu_t - \frac{\gamma^n}{2} (\sigma \varphi_t + \beta_t^n)^2 \right) dt - \lambda(\varphi_T^\uparrow + \varphi_T^\downarrow) \right]. \quad (4.1)$$

We again focus on the long-run average performance $J_T^n(\varphi)/T$ as $T \rightarrow \infty$ of *admissible strategies* that satisfy the integrability condition

$$\mathbb{E} \left[\int_0^T \varphi_t^2 dt \right] < \infty, \quad \mathbb{E}[\varphi_T^\uparrow + \varphi_T^\downarrow] < \infty, \quad (4.2)$$

as well as the transversality condition

$$\lim_{T \rightarrow \infty} \frac{1}{T} \mathbb{E} [|\varphi_T|] = 0. \quad (4.3)$$

4.1 Equilibrium

We use an analogous notion of Radner equilibrium as in Definition 3.2:

Definition 4.1. $\mu \in \mathcal{L}^2$ is a (long-run) equilibrium return if there exist admissible strategies φ^1, φ^2 for agents 1 and 2 such that:

(Market Clearing) The total demand $\varphi^1 + \varphi^2$ matches the supply s of the risky asset at all times;

(Individual Optimality) The strategy φ^n is optimal for the long-run version of agent n 's control problem (4.1) in that,

$$\limsup_{T \rightarrow \infty} \frac{1}{T} [J_T^n(\psi) - J_T^n(\varphi)] \leq 0, \quad \text{for all competing admissible strategies } \psi. \quad (4.4)$$

The construction of the equilibrium return with proportional costs is based on the analogue of the mean-reverting process from Lemma 3.4. This turns out to be a doubly-reflected Brownian motion,

$$dX_t = \delta dW_t + dL_t - dU_t, \quad (4.5)$$

where $X_{0-} = \varphi_{0-}^1 - \frac{s\gamma^2}{\gamma^1 + \gamma^2}$ and L, U are the minimal increasing processes with $L_{0-} = U_{0-} = 0$ that keep $(X_t)_{t \geq 0}$ in the interval $[-l, l]^2$ whose endpoints have the following explicit expression:

$$l = \sqrt[3]{\frac{3\lambda\delta^2}{2\gamma\sigma^2}}, \quad (4.6)$$

where γ and δ are defined as in Lemma 3.3.

With the state variable X at hand, we can now formulate our second main result. It shows that the equilibrium return with proportional costs can be expressed in direct analogy to its counterpart for the smooth, superlinear costs treated in Theorem 3.6. The only difference is that the mean-reverting state variable in Theorem 3.6 is replaced by the doubly-reflected Brownian motion from (4.5).

Theorem 4.2. *With the solution $(X_t)_{t \geq 0}$ of (4.5), define*

$$\mu_t = \bar{\gamma} [s\sigma^2 + \sigma(\beta_t^1 + \beta_t^2)] + \frac{(\gamma^1 - \gamma^2)\sigma^2}{2} X_t, \quad t \geq 0. \quad (4.7)$$

Then, the trading strategies

$$\varphi_t^1 = \varphi_{0-}^1 + L_t - U_t, \quad \varphi_t^2 = \varphi_{0-}^2 + U_t - L_t, \quad t \geq 0, \quad (4.8)$$

clear the market and are individually optimal in the long run. Therefore $(\mu_t)_{t \geq 0}$ is an equilibrium return.

Proof. See Section 8.2. □

Note that, in equilibrium, each agent's singular control problem has a fully explicit solution. Similar closed-form expressions for optimal no-trade regions also obtain for the ergodic control of Brownian motion, which underlies the tractability of problems with *small* transaction costs [44, 32, 11]. Surprisingly, the equilibrium constructed in Theorem 4.2 displays the same tractability, even though the corresponding equilibrium return is not zero but a reflected Brownian motion.

²See [36] for the pathwise construction of L, U . In particular, there is an initial jump in L or U if the initial value X_{0-} lies below $-l$ or above l , respectively. On $(0, T]$, L and U have continuous paths.

5 Calibration

To assess the quantitative properties of our equilibrium returns, we now calibrate the model to price and trading volume data for a typical US stock, American Express (AXP). We use ten years of data from January 2, 2009 to January 2, 2019 available on the Nasdaq website.³

5.1 Calibration of the Frictionless Baseline Model

We first consider the frictionless baseline version of the model from Section 2.2. The exogenous (absolute) volatility σ can be estimated directly from the time series of stock prices, leading to $\sigma = 15.003$ for our AXP dataset.⁴ To obtain a simple parsimonious model for the equilibrium returns, we suppose throughout as in [38] that there is no aggregate endowment ($\beta_t^1 = -\beta_t^2 = \sigma \delta W_t$). Then, the frictionless equilibrium expected return from (2.2) is $\bar{\mu} = \bar{\gamma} s \sigma^2$. As the number of shares outstanding is $s = 854262000$,⁵ we choose $\bar{\gamma} = 3.971 \times 10^{-11}$ to match this to the average (absolute) yearly returns of 7.635 in the AXP time series.

5.2 Calibration with Transaction Costs

Whereas the frictionless equilibrium price only depends on the aggregate risk aversion $\bar{\gamma} = \frac{\gamma^1 \gamma^2}{\gamma^1 + \gamma^2}$ and aggregate endowment $\beta^1 + \beta^2$, the individual values of these parameters need to be pinned down to determine equilibria with transaction costs. Moreover, the initial allocations for the agents need to be specified and an appropriate estimate for the respective trading cost is evidently needed.

Proportional Costs For proportional costs, we use the AXP bid-ask spread quoted on BATS on Dec. 21, 2018 as a proxy: $\lambda_1 = 1.05$.⁶ Once the aggregate risk aversion $\bar{\gamma}$ is fixed, the individual agents' absolute risk aversions γ^1, γ^2 are free parameters in the present model, which correspond to the agents' sizes relative to each other. If both agents are of the same size, the frictional equilibrium coincides with its frictionless counterpart. To illustrate the effect of heterogeneity, we set $\gamma^1 = 2\gamma^2$, so that the larger agent 2 has twice the risk capacity of agent 1. Then, with $\bar{\gamma} = 3.971 \times 10^{-11}$ we have $\gamma^1 = 1.191 \times 10^{-10}$, $\gamma^2 = 5.956 \times 10^{-11}$, and $\gamma = (\gamma^1 + \gamma^2)/2 = 8.934 \times 10^{-11}$. For the initial allocations, we suppose that $\varphi_{0-}^1 = \varphi_{0-}^2 = s/2$.

Finally, we calibrate the value of the endowment volatilities $\beta_1^1 = -\beta_1^2 = \delta_1 \sigma$ to time-series data for trading volume. More specifically, we choose the parameter δ_1 to match the average yearly share turnover in 2009-2018, $\text{ShTu} = 1794406220$ (that is, about 210% of the outstanding shares),⁷ to the corresponding long-term average value in our model. Using the ergodic theorem, the latter can be calculated as in [23, Lemma C.2],

$$\text{ShTu} = \lim_{T \rightarrow \infty} \frac{1}{T} \int_0^T d|\varphi|_t = \lim_{T \rightarrow \infty} \frac{L_T}{T} + \lim_{T \rightarrow \infty} \frac{U_T}{T} = \frac{\delta_1^2}{2l} = \left(\frac{\gamma \sigma^2}{12\lambda_1} \right)^{1/3} \delta_1^{4/3} \quad \text{a.s.}$$

Accordingly, we have

$$\delta_1 = \left(\frac{\text{ShTu}^3 12\lambda_1}{\gamma \sigma^2} \right)^{\frac{1}{4}} = 1.379 \times 10^9, \quad \text{so that } \beta_1^1 = -\beta_1^2 = \delta_1 \sigma = 2.069 \times 10^{10}.$$

³See <https://www.nasdaq.com/symbol/axp>.

⁴For the stock prices around 100 in our time series, this corresponds to a Black-Scholes volatility of around 15%.

⁵See <https://www.nasdaq.com/symbol/axp/stock-report>.

⁶Since the corresponding stock price was approximately 100, this corresponds to a relative bid-ask spread of around 1%, in line with the parameter values used in [39, 10], for example.

⁷See <https://www.nasdaq.com/symbol/axp/historical?tf=10y>.

Superlinear Costs For comparison, we also consider the power costs $G_q(x) = \lambda_q|x|^q/q$, $q \in (1, 2]$. In this case, the ergodic theorem shows that the long-term average share turnover per year is

$$\text{ShTu} = \lim_{T \rightarrow \infty} \frac{1}{T} \int_0^T |\dot{\varphi}_t^1| dt = \int_{-\infty}^{\infty} |(G'_q)^{-1}[g_q(x)]| \nu_q(x) dx \quad \text{a.s.}$$

Here, $\nu_q(x)$ is the invariant density of the stationary law of the state variable X . For quadratic costs $G_2(x) = \lambda_2 x^2/2$, this is an Ornstein-Uhlenbeck process (cf. Remark 3.5) whose stationary distribution is Gaussian with mean zero and variance $\delta_2^2/2\sqrt{\gamma\sigma^2/\lambda_2}$. As $(G'_2)^{-1}[g(x)] = -\sqrt{\gamma\sigma^2/\lambda_2}x$, the average turnover per year in turn is proportional to δ_2 in this case,

$$\lim_{T \rightarrow \infty} \frac{1}{T} \int_0^T |\dot{\varphi}_t^1| dt = \sqrt{\frac{\gamma\sigma^2}{\lambda_2}} \sqrt{\frac{2}{\pi}} \frac{\delta_2}{\sqrt{2} \sqrt{\gamma\sigma^2/\lambda_2}} = \left(\frac{\gamma\sigma^2}{\pi^2 \lambda_2}\right)^{1/4} \delta_2 \quad \text{a.s.}$$

Accordingly, we have $\delta_2 = \text{ShTu}/(\frac{\gamma\sigma^2}{\pi^2 \lambda_2})^{1/4}$, and it remains to choose an appropriate value for the trading cost parameter λ_2 . To make its impact comparable to the proportional cost, we choose it to obtain the same stationary variance of the state variable X as with proportional costs. With proportional costs, this process has a uniform stationary law with standard deviation $l/\sqrt{3}$. With quadratic costs, the stationary standard deviation of the Ornstein-Uhlenbeck state variable is $\delta_2/\sqrt[4]{4\gamma\sigma^2/\lambda_2} = \text{ShTu}\sqrt{\pi\lambda_2}/\sqrt{2\gamma\sigma^2}$. To match this with the stationary standard deviation for proportional costs, we choose $\lambda_2 = 3.725 \times 10^{-10}$. This leads to $\delta_2 = 1.173 \times 10^9$, and hence $\beta_2^1 = \beta_2^2 = \delta_2\sigma = 1.760 \times 10^{10}$. Note that his value is substantially smaller than direct estimates for quadratic costs used in [21, 12], for example. Whence, the value we use here should lead to conservative lower bound for the corresponding equilibrium effects of actual superlinear trading costs.

For general power costs $G_q(x) = \lambda_q|x|^q/q$ the solution g_q of the ODE (3.5) is not known explicitly. However, by exploiting the homotheticity of the power function, a change of variable allows to reduce (3.5) to an equation that only depends on the elasticity q of the price impact function, but not the parameters λ_q , δ_q that we are trying to determine here. Accordingly, the values of λ_q , δ_q that match the average share turnover observed empirically as well as the variance of the state variable for proportional costs can be expressed as integrals of this universal function. For fixed q , these can in turn be computed by using a quadrature formula to integrate the numerical solution of (3.5), cf. Appendix B for more details.

For $q = 1.5$ (which is in line with empirical estimates of actual trading costs in [4, 37]), this leads to

$$\delta_{1.5} = 1.252 \times 10^9, \quad \lambda_{1.5} = 1.78 \times 10^{-5},$$

and in turn

$$\beta_{1.5}^1 = -\beta_{1.5}^2 = 1.879 \times 10^{10}.$$

Simulations of the equilibrium returns (generated with the same Brownian sample path) for these three sets of parameters are shown in Figure 1. The corresponding model turnover for $q = 2$ and $q = 3/2$ is compared to the historical trading volume data in Figure 2. Clearly, both simulations broadly agree with the level and mean-reverting dynamics observed in the data. However, the small differences between the corresponding state variables depicted in Figure 1 are magnified by the application of the function $|(G'_q)^{-1}(g_q(\cdot))|$, cf. Figure 2. Indeed, periods with very high and low turnover are substantially more common with subquadratic costs, in line with the empirical data.

6 More General Settings and Nonlinear FBSDEs

We now discuss how the results from the previous sections formally extend to more general settings with a finite time horizon, more general state dynamics, and endogenous volatilities. Corresponding verification results would require wellposedness for non-linear, fully-coupled systems of FBSDEs. For quadratic trading costs and sufficiently similar risk aversions of the two agents, such results are developed in [29]. Extensions to more general trading costs are an intriguing but challenging direction for further research. This is beyond our scope here; however, we discuss numerical algorithms based on the deep-learning approach of [28] in Section 7 below.

6.1 General Market

In this section, we consider more general state dynamics where, for $n = 1, 2$, the cumulative endowment is of the form

$$d\zeta_t^n = \beta_t^n dW_t, \quad \text{for a general } \beta^n \in \mathcal{L}^2,$$

and the price of the risky asset has dynamics

$$dS_t = \mu_t dt + \sigma_t dW_t. \quad (6.1)$$

Now, not just the equilibrium return process $\mu \in \mathcal{L}^1$ but also the initial price $S_0 \in \mathbb{R}$ and the volatility process $\sigma \in \mathcal{L}^2$ are to be determined in equilibrium by matching the agents demand to the supply $s \in \mathbb{R}$ of the risky asset. To pin down these additional quantities, we assume as in [29] that the terminal stock price is given by an exogenous \mathcal{F}_T -measurable random variable:

$$S_T = \mathfrak{S}. \quad (6.2)$$

This can be interpreted as a fundamental value or as a terminal dividend.

6.2 Frictionless Optimization and Equilibrium

The frictionless results from Section 2 readily adapt this more general setting. Indeed, also for a general stochastic volatility process, pointwise maximization of the goal functional (2.1) still yields the agents' individually optimal strategies,

$$\varphi_t^n = \frac{\mu_t}{\gamma^n \sigma_t^2} - \frac{\beta_t^n}{\sigma_t}, \quad t \in [0, T].$$

The equilibrium return is then still pinned down by matching the agents' total demand $\varphi_t^1 + \varphi_t^2$ to the supply s of the risky asset:

$$\bar{\mu}_t = \bar{\gamma} [s \bar{\sigma}_t^2 + \bar{\sigma}_t (\beta_t^1 + \beta_t^2)], \quad t \in [0, T], \quad \text{where } \bar{\gamma} = \frac{\gamma^1 \gamma^2}{\gamma^1 + \gamma^2}. \quad (6.3)$$

Now, however, we also need to determine the corresponding initial price of the risky asset and its volatility. To this end, insert (6.3) into (6.1) and recall the terminal condition (6.2). This leads the following scalar quadratic BSDE:

$$d\bar{S}_t = \bar{\gamma} [s \bar{\sigma}_t^2 + \bar{\sigma}_t (\beta_t^1 + \beta_t^2)] dt + \bar{\sigma}_t dW_t, \quad \bar{S}_T = \mathfrak{S}. \quad (6.4)$$

As is well known, the solution of this equation can be expressed in terms of the Laplace transform of the terminal condition, leading to explicit solutions in many concrete examples [29, Section 4.1].

Example 6.1. If

$$\beta^1 + \beta^2 = 0 \quad \text{and} \quad \mathfrak{S} = bT + aW_T,$$

then the frictionless equilibrium price \bar{S} is a Bachelier model with constant expected returns and volatilities:

$$\bar{S}_t = (b - s\bar{\gamma}a^2)T + s\bar{\gamma}a^2t + aW_t, \quad t \in [0, T],$$

Agents $n = 1, 2$'s optimal trading strategies in this frictionless equilibrium are

$$\bar{\varphi}_t^n = \frac{s\bar{\gamma}}{\gamma^n} - \frac{\beta_t^n}{a}, \quad t \in [0, T]. \quad (6.5)$$

6.3 Frictional Optimization and Equilibrium

With transaction costs, both individual optimization and the corresponding equilibria become significantly more involved, leading to systems of fully-coupled nonlinear FBSDEs. Let us first consider the agents' individual optimization problems for a given initial asset price $S_0 \in \mathbb{R}$, expected returns process $(\mu_t)_{t \in [0, T]}$ and volatility process $(\sigma_t)_{t \in [0, T]}$. By strict convexity of the goal functional (2.1), optimality is equivalent to the first-order condition that the Gateaux derivative $\lim_{\rho \rightarrow 0} \frac{1}{\rho} (J_T^n(\dot{\varphi} + \rho\psi) - J_T^n(\dot{\varphi}))$ vanishes for *any* perturbation ψ , cf. [20]:

$$0 = \mathbb{E}_t \left[\int_0^T \left(\mu_t \int_0^t \psi_u du - \gamma^n \sigma_t (\sigma_t \varphi_t + \beta_t^n) \int_0^t \psi_u du - G'(\dot{\varphi}_t) \dot{\psi}_t \right) dt \right].$$

As in [7], this can be rewritten using Fubini's theorem as

$$0 = \mathbb{E}_t \left[\int_0^T \left(\int_t^T (\mu_u - \gamma^n \sigma_u (\sigma_u \varphi_u + \beta_u^n)) du - G'(\dot{\varphi}_t) \right) \dot{\psi}_t dt \right].$$

Since this has to hold for *any* perturbation $\dot{\psi}_t$, the tower property of conditional expectation yields

$$G'(\dot{\varphi}_t) = \mathbb{E}_t \left[\int_t^T \mu_u - \gamma^n \sigma_u (\sigma_u \varphi_u + \beta_u^n) du \right] = M_t - \int_0^t (\mu_u - \gamma^n \sigma_u (\sigma_u \varphi_u + \beta_u^n)) du, \quad (6.6)$$

for a martingale $M = M_0 + \int_0^\cdot Z_t dW_t$ that needs to be determined as part of the solution. Itô's formula applied to $(G')^{-1}$ in turn shows that agent n 's optimal position φ^n and the corresponding trading rate $\dot{\varphi}^n$ solve the following *nonlinear* FBSDE:

$$d\varphi_t^n = \dot{\varphi}_t^n dt, \quad \varphi_0^n = \varphi_{0-}^n, \quad (6.7)$$

$$d\dot{\varphi}_t^n = Z_t^n dW_t + \frac{1}{G''(\dot{\varphi}_t^n)} \left(\gamma^n \sigma_t (\sigma_t \varphi_t^n + \beta_t^n) - \mu_t - \frac{1}{2} G'''(\dot{\varphi}_t^n) (Z_t^n)^2 \right) dt, \quad \dot{\varphi}_T^n = 0. \quad (6.8)$$

Note that for the quadratic costs $G(x) = \lambda x^2/2$ considered in [29], the generator of the backward component does not depend on its volatility and itself. If the volatility is constant, the backward equation then becomes linear and can in turn be solved by reducing it to some standard Riccati equations [7, 9]. For stochastic volatilities, these are replaced by a backward *stochastic* Riccati equation, compare [35, 6]. With nonlinear costs, no such simplifications are possible. In fact, the wellposedness of the system is unclear even for short time horizons since no Lipschitz condition is satisfied for costs of power form $G(x) = \lambda|x|^q/q$, $q \in (1, 2)$, for example.

Despite these difficulties, solving for the corresponding equilibrium return is – surprisingly – not more difficult than for quadratic costs. To see this, plug both agents' optimality conditions (6.8) into the market clearing condition $\dot{\varphi}^1 + \dot{\varphi}^2 = 0$. This gives

$$0 = (Z_t^1 + Z_t^2)dW_t + \frac{1}{G''(\dot{\varphi}_t^1)} \left(\gamma^1 \sigma_t (\sigma_t \varphi_t^1 + \beta_t^1) - \mu_t - \frac{1}{2} G'''(\dot{\varphi}_t^1) (Z_t^1)^2 \right) dt \\ + \frac{1}{G''(\dot{\varphi}_t^2)} \left(\gamma^2 \sigma_t (\sigma_t \varphi_t^2 + \beta_t^2) - \mu_t - \frac{1}{2} G'''(\dot{\varphi}_t^2) (Z_t^2)^2 \right) dt.$$

Whence, $Z^2 = -Z^1$. Moreover, in equilibrium we necessarily have $\varphi^2 = s - \varphi^1$, $\dot{\varphi}^2 = -\dot{\varphi}^1$, so that

$$\mu_t = \frac{\sigma_t}{2} [s\sigma_t\gamma^2 + \gamma^1\beta_t^1 + \gamma^2\beta_t^2 + (\gamma^1 - \gamma^2)\sigma_t\varphi_t^1], \quad (6.9)$$

since the trading cost $G(x)$ is symmetric. This is exactly the same formula as for quadratic costs in [29]. Plugging this expression back into agent 1's optimality condition (6.6) in turn yields a backward equation that is linear in the optimal position, like for quadratic costs:⁸

$$dY_t = dG'(\dot{\varphi}_t^1) = Z_t^1 dW_t + \frac{\sigma_t}{2} ((\gamma^1 + \gamma^2)\sigma_t\varphi_t^1 - s\gamma^2\sigma_t + \gamma^1\beta_t^1 - \gamma^2\beta_t^2) dt, \quad Y_T = 0, \quad (6.10)$$

where the terminal condition comes from $Y_T = G'(0) = 0$. All nonlinearities are absorbed into the corresponding forward component,

$$d\varphi_t^1 = (G')^{-1}[Y_t]dt, \quad \varphi_0^1 = \varphi_{0-}^1. \quad (6.11)$$

If the volatility process σ is not given exogenously, it needs to be determined from the terminal condition \mathfrak{S} . By plugging expression (6.9) for the equilibrium return into the price dynamics (6.1), we obtain the following BSDE, which is coupled to the forward-backward system (6.10-6.11):

$$dS_t = \frac{\sigma_t}{2} [s\sigma_t\gamma^2 + \gamma^1\beta_t^1 + \gamma^2\beta_t^2 + (\gamma^1 - \gamma^2)\sigma_t\varphi_t^1] dt + \sigma_t dW_t, \quad S_T = \mathfrak{S}. \quad (6.12)$$

This is again the same equation as for quadratic costs [29]. In particular, if both agents' risk aversions coincide ($\gamma^1 = \gamma^2$), it decouples from the forward-backward system (6.10-6.11) and leads to the same equilibrium price as without transaction costs. For heterogenous but sufficiently similar risk aversions $\gamma^1 \approx \gamma^2$ and quadratic costs, it is shown in [29] that a solution of (6.10-6.12) exists and identifies an equilibrium with transaction costs. However, the proof crucially exploits that with quadratic costs, the forward-backward system (6.10-6.11) for a given volatility process $(\sigma_t)_{t \in [0, T]}$ can be studied by means of the stochastic Riccati equation from [35]. Establishing such results for more general trading costs – where such tools are not available – is a challenging direction for further research.

Here, let us just briefly sketch how the nonlinear FBSDE (6.10-6.12) reduces to a nonlinear ODE in the context of Section 3, where the endowment volatilities $\beta_t^n = \beta^n W_t$, $n = 1, 2$ follow Brownian motions. As in Lemma 3.3, define

$$\gamma = \frac{\gamma^1 + \gamma^2}{2}, \quad \delta = \frac{\gamma^1\beta^1 - \gamma^2\beta^2}{(\gamma^1 + \gamma^2)\sigma}.$$

⁸Here, these linear dynamics obtain if this equation is expressed in terms of $G'(\dot{\varphi}^1)$ rather than $\dot{\varphi}^1$. In contrast, we need to work with the dynamics of $\dot{\varphi}^n$ to derive the market clearing condition.

Since the volatility process is exogenous and constant there, we don't have to deal with the second backward component (6.12) and, moreover, can work with the state variable

$$X_t := \varphi_t^1 - \frac{s\gamma^2}{\gamma^1 + \gamma^2} + \frac{\gamma^1\beta_t^1 - \gamma^2\beta_t^2}{(\gamma^1 + \gamma^2)\sigma}.$$

With this notation, the forward-backward system (6.10-6.11) becomes autonomous,

$$dX_t = (G')^{-1}[Y_t]dt + \delta dW_t, \quad X_0 = \varphi_{0-}^1 - \frac{s\gamma^2}{\gamma^1 + \gamma^2}, \quad (6.13)$$

$$dY_t = \gamma\sigma^2 X_t dt + Z_t^1 dW_t, \quad Y_T = 0. \quad (6.14)$$

Now use the standard ansatz that the backward component Y_t should be a function $g(t, X_t)$ of time and the forward component. It's formula and the dynamics of the forward component in turn yield

$$dY_t = dg(t, X_t) = \left(g_t(t, X_t) + g_x(t, X_t)(G')^{-1}[g(t, X_t)] + \frac{\delta^2}{2}g_{xx}(t, X_t) \right) dt + \delta g_x(t, X_t)dW_t.$$

Comparing the drift rate to the BSDE (6.10), we therefore obtain the following semilinear PDE:

$$g_t(t, x) + g_x(t, x)(G')^{-1}[g(t, x)] + \frac{\delta^2}{2}g_{xx}(t, x) = \gamma\sigma^2 x. \quad (6.15)$$

For a long time horizon, the solution should become stationary ($g_t(t, x) \approx 0$). This leads to the nonlinear ODE from Lemma 3.3:

$$\frac{\delta^2}{2}g''(x) + g'(x)(G')^{-1}[g(x)] = \gamma\sigma^2 x.$$

For finite time horizons, where the PDE (6.15) cannot be reduced to an ODE, it is natural to expect that the correct solution still should be identified by the same growth condition in the x -variable. However, with a finite time horizon, these bounds will be a strict near maturity. Therefore solving the corresponding equations numerically – which is not straightforward already in the ODE case – becomes difficult in this case.

As a remedy, in the next section we therefore propose a numerical algorithm in the spirit of [28]. It solves the FBSDE by simulation and therefore bypasses the need to identify the correct boundary conditions. The algorithm approximates the dependence of the backward component on the forward components by a deep neural network. Whence, it is also able to handle higher-dimensional settings, e.g., with endogenous volatilities, random and time-varying transaction costs, etc.

7 Numerics

We now present a numerical algorithm to solve the FBSDEs from Section 6. The algorithm is then tested for the calibrated parameters from Section 5.

7.1 Deep-Learning Algorithm

Overview Solving the forward-backward system is challenging because it is multidimensional and the forward and backward components are fully coupled. Nevertheless, it is amenable to the

simulation-based approach of [28], which approximates the solution by a deep neural network. In [28] the focus lies on BSDEs, but the approach can readily be extended to FBSDEs.

Let us briefly sketch the main idea; further details on the implementation are provided below. The first step is to pass to a time-discretized version of (6.10-6.12), e.g., using the Euler scheme. Solving this system amounts to finding at each time step t_k the unknown ‘‘controls’’ Z_{t_k}, σ_{t_k} . If the terminal condition is a function $\mathfrak{S}(W_T)$ of the underlying Brownian motion only as in Example 6.1, then it is well known that the solution and in turn Z_{t_k}, σ_{t_k} are functions of the forward variables, $Z_{t_k} = F_k^{\theta^Z}(W_{t_k}, \varphi_{t_k}^1)$ and $\sigma_{t_k} = F_k^{\theta^\sigma}(W_{t_k}, \varphi_{t_k}^1)$.

The algorithm of [28] approximates each of these functions with a function in the class $\{F^{\bar{\theta}}: \bar{\theta} \in \Theta\}$ of neural networks, where we write $\theta = (\theta_0^Y, \theta_0^S, \theta_0^\sigma, \dots, \theta_n^\sigma, \theta_0^Z, \dots, \theta_n^Z)$ for the collection of all the corresponding parameters. The goal now is to choose these parameters in order to match the terminal conditions $Y_T = 0$ and $S_T = \mathfrak{S}(W_T)$ of the system sufficiently well. To this end, one starts with an initial guess for the network functions and then simulates the system forward in time. In this way, a simulated Brownian sample path is mapped to a corresponding terminal condition. This mapping can be viewed as a deep neural network, which is determined by the choice of the building block networks $\{F^{\bar{\theta}}: \bar{\theta} \in \Theta\}$ (i.e., two networks of type (7.5) for each time-step) and the FBSDE system, which describes how these building block networks are concatenated over time (see (7.2) below). To iteratively update the network functions until the terminal conditions are matched sufficiently well, one may then leverage computational technology available for such networks, such as backpropagation and stochastic gradient descent-type algorithms, see e.g. [24, Chapters 6 and 8]. This can be implemented efficiently, e.g., in Python using Tensorflow.

Algorithm Let us now describe the approximation algorithm in more detail. Fix a discrete time grid $0 = t_0 < t_1 < \dots < t_n = T$. For any choice of parameter θ , consider the following discrete-time forward system obtained by discretizing (6.10-6.12): starting from initial values $\varphi_0^\theta = \varphi_0^1$, $Y_0^\theta = \theta_0^Y$, $S_0^\theta = \theta_0^S$, for $k = 0, \dots, n-1$ calculate

$$Z_{t_k}^\theta = F_k^{\theta^Z}(W_{t_k}, \varphi_{t_k}^\theta), \quad \sigma_{t_k}^\theta = F_k^{\theta^\sigma}(W_{t_k}, \varphi_{t_k}^\theta), \quad (7.1)$$

and step forward according to the Euler scheme

$$\begin{aligned} \varphi_{t_{k+1}}^\theta &= \varphi_{t_k}^\theta + (G')^{-1}(Y_{t_k}^\theta)(t_{k+1} - t_k), \\ Y_{t_{k+1}}^\theta &= Y_{t_k}^\theta + \frac{\sigma_{t_k}^\theta}{2} \left[\sigma_{t_k}^\theta \varphi_{t_k}^\theta (\gamma^1 + \gamma^2) - \sigma_{t_k}^\theta s \gamma^2 + \gamma^1 \beta_{t_k}^1 - \gamma^2 \beta_{t_k}^2 \right] (t_{k+1} - t_k) + Z_{t_k}^\theta (W_{t_{k+1}} - W_{t_k}), \\ S_{t_{k+1}}^\theta &= S_{t_k}^\theta + \frac{\sigma_{t_k}^\theta}{2} \left[s \sigma_{t_k}^\theta \gamma^2 + (\gamma^1 - \gamma^2) \sigma_{t_k}^\theta \varphi_{t_k}^\theta + \gamma^1 \beta_{t_k}^1 + \gamma^2 \beta_{t_k}^2 \right] (t_{k+1} - t_k) + \sigma_{t_k}^\theta (W_{t_{k+1}} - W_{t_k}). \end{aligned} \quad (7.2)$$

For any choice of the approximation parameter θ , this defines a discrete-time stochastic process, but of course the terminal conditions $Y_T^\theta = 0$ and $S_T^\theta = \mathfrak{S}(W_T)$ will not even be approximately satisfied for an arbitrary choice of θ . However, if $\hat{\theta}$ is a minimizer of

$$\min_{\theta} \mathcal{L}(\theta), \quad \text{where } \mathcal{L}(\theta) = \mathbb{E}[(Y_T^\theta)^2] + \mathbb{E}[(S_T^\theta - \mathfrak{S})^2], \quad (7.3)$$

where the number n of time steps is sufficiently large and the function class $\{F^{\bar{\theta}}: \bar{\theta} \in \Theta\}$ is sufficiently rich, then $(\varphi^{\hat{\theta}}, Y^{\hat{\theta}}, S^{\hat{\theta}})$ should be a good approximation for the solution (φ^1, Y, S) of (6.10-6.12) at the time-points t_0, \dots, t_n .

The minimization problem (7.3) can be tackled using the ‘‘stochastic gradient descent algorithm’’. The main idea is the following: if the objective functional \mathcal{L} was known explicitly and

differentiable, then the classical gradient descent algorithm could be applied. That is, starting from an initial guess $\theta^{(0)}$, one iteratively updates

$$\theta^{(j+1)} = \theta^{(j)} - \eta_j \nabla \mathcal{L}_j(\theta^{(j)}), \quad (7.4)$$

where $\mathcal{L}_j = \mathcal{L}$ and the learning rate $\eta_j > 0$ is fixed ($\eta_j = \eta$ for all j) or decreasing to 0. Under suitable assumptions on \mathcal{L} and $\{\eta_j\}_{j \in \mathbb{N}}$ the parameter $\theta^{(j)}$ then converges to a (local) minimum of \mathcal{L} as $j \rightarrow \infty$. However, since \mathcal{L} is not known explicitly, one applies the *stochastic* gradient descent algorithm, which is the same procedure as just described, but approximates the expectations in \mathcal{L} by a sample average in each iteration j ,

$$\mathcal{L}_j(\theta) = \frac{1}{N_b} \sum_{i=1}^{N_b} (Y_T^\theta(W^i))^2 + (S_T^\theta(W^i) - \mathfrak{S}(W^i))^2.$$

Here, $N_b \in \mathbb{N}$ is called the “batch size” and $Y_T^\theta(W^i)$, $S_T^\theta(W^i)$ are calculated by plugging independent Brownian motions W^1, \dots, W^{N_b} into the Euler scheme (7.1-7.2).

In order to use this to apply the updating rule (7.4), one needs to be able to calculate $\nabla \mathcal{L}_j(\theta)$ efficiently and this is the point at which the choice of $\{F^{\bar{\theta}}: \bar{\theta} \in \Theta\}$ becomes crucial. As is apparent from (7.1-7.2), the dependence of the solution on the parameter θ is complex, since the state variables and parametric functions are iteratively added, multiplied and composed. For instance $Z_{t_k}^\theta$ depends not only on θ_k^Z , but also (via $\varphi_{t_k}^\theta$) on $\theta_0^Z, \dots, \theta_{k-2}^Z$ and $\theta_0^\sigma, \dots, \theta_{k-2}^\sigma$. This makes the computational solution of (7.3) by classical numerical techniques highly challenging. Whence, while in principle any sufficiently rich parametric family of functions could be chosen for $\{F^{\bar{\theta}}: \bar{\theta} \in \Theta\}$ in the scheme described above, it turns out to be particularly useful to choose a class of neural networks here. Then, Y_T^θ and S_T^θ can be viewed as the outputs of a deep neural network with random input $(W_{t_k})_{k=0, \dots, n}$. Thanks to the compositional structure of neural networks one can then use the chain rule to calculate the gradient $\nabla \mathcal{L}_j(\theta)$ in closed form. Furthermore, the resulting analytical expressions can be evaluated efficiently using the so-called backpropagation algorithm, see, e.g., [24]. By using subgradients, this also extends to e.g. the “ReLU activation function” used below. Finally, all of this can be implemented efficiently in the computational graph structure employed in libraries such as Tensorflow or Torch.

In summary, the learning algorithm iteratively updates the network parameters θ until a desired approximation accuracy is reached for some $\hat{\theta}$. Note that the accuracy of the approximation can be verified out of sample (e.g., in the numerical experiments in Section 7.2) by simulating a large number N_{test} of additional independent sample paths of W and evaluating the empirical loss $\mathcal{L}_j(\hat{\theta})$ (with $N_b = N_{\text{test}}$) on this collection of test paths.

Implementation For the numerical experiments in Section 7.2, each $F^{\bar{\theta}}$ is a neural network with two hidden layers. For the activation function we choose the popular Rectified Linear Unit (*ReLU*) ρ , which applies $x \mapsto \max(x, 0)$ to each component of a vector. Denoting by $N_1, N_2 \in \mathbb{N}$ the number of nodes in the hidden layer, we thus consider functions of the form

$$F^{\bar{\theta}}(x) = A^2 \rho(A^1 \rho(A^0 x + b^0) + b^1), \quad x \in \mathbb{R}^2, \quad (7.5)$$

where $A^0 \in \mathbb{R}^{N_1 \times 2}$, $b^0 \in \mathbb{R}^{N_1}$, $A^1 \in \mathbb{R}^{N_2 \times N_1}$, $b^1 \in \mathbb{R}^{N_2}$, $A^2 \in \mathbb{R}^{1 \times N_2}$ are called the *weights* and *biases* of the network and we denote by Θ the set of all parameters $\bar{\theta} = (A^0, b^0, A^1, b^1, A^2)$. To find a close-to-optimal parameter $\hat{\theta}$ in (7.3) we randomly initialize the network parameters and subsequently use the Adam algorithm [30], which is a variant of stochastic gradient descent which adaptively adjusts the learning rates for all network parameters. Here, some initial hyperparameter

optimization has led us to choose $N_1 = N_2 = 15$, set the initial learning rate to 0.0005 and use a batch size of 128. In order to accelerate the parameter training procedure, we apply batch-normalization [34] (see also [24, Section 8.7.1]) at different stages: before the input is fed into the network, before applying the activation function ρ and after the last linear transformation A^2 . All computations are performed in Python using Tensorflow.

7.2 Numerical results

The algorithm introduced in Section 7.1 is now applied to solve the forward-backward equations corresponding to Example 6.1 from Section 6. As a sanity check, we first consider the simplest version of the model, where the price volatility is exogenous. In this setting, we compare the numerical solution to the nonlinear ODE that describes the exact solution of the infinite-horizon version of the model.

Subsequently, we consider the model with endogenous volatility. In order to test the performance of the learning algorithm in this case, we compare its results to the semi-explicit solution in term of Riccati equations obtained for quadratic costs in [29].

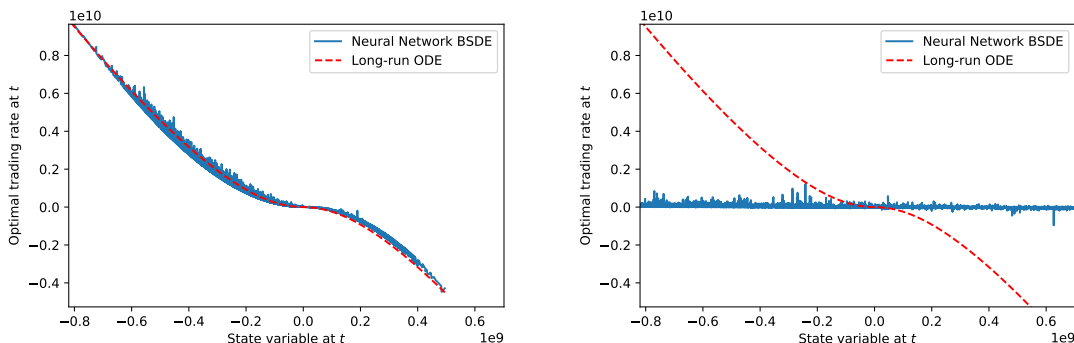


Figure 5: Comparison of the long-run optimal trading rate to the neural-network approximation of its finite horizon counterpart for power costs with $q = 1.5$ and $t = T - t_k = 0.2$ (left panel) and $t = T - t_k = 0.01$ (right panel).

Exogenous volatility We first consider the finite-horizon version of the model from Section 3 with power costs $G_q(x) = \lambda_q |x|^q / q$, where $q = 1.5$, $\varphi_0^0 = \varphi_0^1 = s/2$ and the model parameters are calibrated as in Section 5. The algorithm described in Section 7.1 for the general FBSDE (6.10-6.12) can be readily adapted by setting $\sigma_{t_k}^\theta = \sigma$ for all k , only considering the first two equations in (7.2), and minimizing $\mathbb{E}[(Y_T^\theta)^2]$. An alternative, slightly more efficient approach is to use instead the system (6.13), (6.14) and discretize it analogously to (7.2). The algorithm from Section 7.1 in turn yields a parameter $\hat{\theta}$ such that $(X^{\hat{\theta}}, Y^{\hat{\theta}})$ approximately solves (6.13-6.14). This allows us to generate approximate samples of (6.13-6.14) by simulating sample paths of W and evaluating $(X^{\hat{\theta}}, Y^{\hat{\theta}})$. On the other hand we know that $Y_{t_k} = g(t_k, X_{t_k})$, where g solves (6.15). Thus we generate $N_{\text{test}} = 10^6$ samples of W , evaluate $(X^{\hat{\theta}}, Y^{\hat{\theta}})$ on each of them and obtain an approximation $\hat{g}(t_k, x)$ of $g(t_k, x)$ by assigning to each point x which is attained by a sample of $X_{t_k}^{\hat{\theta}}$ the associated sample of $Y_{t_k}^{\hat{\theta}}$. This yields an approximation of the solution to (6.15) on a (random) grid specified by the state variable. According to (6.11), the corresponding optimal trading rate is in turn obtained by applying $(G'_q)^{-1}(\hat{g}(t_k, \cdot))$ to the state variable.

We now compare this to the long-run optimal trading rate from Theorem 3.6, where g is given by the solution of the nonlinear ODE from Lemma 3.3. Figure 5 shows the graph of both functions at $t = T - t_k = 0.2$ and at $t = T - t_k = 0.01$, i.e., the samples of $(X_{t_k}^{\hat{\theta}}, (G'_q)^{-1}(Y_{t_k}^{\hat{\theta}})) = (X_{t_k}^{\hat{\theta}}, (G'_q)^{-1}(\hat{g}(t_k, X_{t_k}^{\hat{\theta}})))$ and $(X_{t_k}^{\hat{\theta}}, (G'_q)^{-1}(g(X_{t_k}^{\hat{\theta}})))$. We observe that the long-run optimum is already very close to the numerical-solution of the finite-horizon problem even for a time horizon of just less than a quarter of a year. On the one hand, this justifies the use of the long-run model as a tractable approximation of its finite-horizon counterpart. On the other hand, it demonstrates that the deep learning algorithm indeed converges to the correct solution in this simplest version of the model.

Endogenous volatility We now turn to the model with endogenous volatility from Section 6. We consider $G_q(x) = \lambda_q|x|^q/q$ both for $q = 2$ (quadratic costs) and $q = 1.5$ (power costs). For λ_q , γ_1 , γ_2 , and $\beta^1 = -\beta^2$ we use the same parameter values as for the model with exogenous volatility (cf. Section 5) and we also again set $\varphi_{0-}^0 = \varphi_{0-}^1 = s/2$. The additional parameters a and b are calibrated to the frictionless equilibrium from Section 6.2. To wit, a is estimated from the time series (resulting in the same value as for σ in Section 5.1) and b is chosen so that $\bar{S}_0 = (b - s\bar{\gamma}a^2)T$ matches the current stock price. We focus on a short time horizon $T = 0.2$ discretized into $n = 100$ time steps.

The deep-learning algorithm from Section 7.1 in turn yields an approximate solution of the forward-backward system (6.10-6.12). To assess the effect of different transaction costs we compare the equilibrium price and volatility to the respective quantity in the frictionless equilibrium, i.e. we examine (sample paths of) the price difference $S^{\hat{\theta}} - \bar{S}$ and the volatility difference $\sigma^{\hat{\theta}} - a$ over time. For quadratic costs it has been shown in [29] that optimal trading rates and the equilibrium price can be described in terms of a system of coupled Riccati ODEs. This provides a benchmark in the case of quadratic costs. The left panels in Figures 1 and 3 show two sample paths of the price and volatility differences for quadratic costs calculated by both methods, i.e., by applying the neural network based algorithm described above and by solving the system of ODEs derived in [29]. Evidently, the neural network based method provides a very accurate approximation of the equilibrium quantities.

The analogous plots for power costs with $q = 1.5$ are shown in the right panels of Figures 3 and 4 (in order to compare these to the corresponding results for quadratic costs, we use the same Brownian paths in each case). Note that no benchmark is available in this case. At least for the short time horizons considered here, the equilibrium prices for the two cost specifications turn out to be very similar. This corroborates the findings from Section 5 and suggests that quadratic costs can also serve as useful proxies for other less tractable costs specifications in settings with endogenous volatilities.

8 Proofs

8.1 Proofs for Section 3

Proof of Lemma 3.4. Strong existence and uniqueness follow from a standard localization argument, cf. [13, Proof of Proposition 1.1]. By Lemma 3.3, we have $g(x) \leq 0$ for $x > 0$ and, in view of Assumption 3.1(ii) there exists $K > 0$ such that

$$|(G')^{-1}(x)| \geq \frac{c}{2}|x| \quad \text{for } |x| \geq |K|.$$

As $(G')^{-1}$ is odd, it follows that, for x such that $|g(x)| \geq K$,

$$x(G')^{-1}(g(x)) = -|x|(G')^{-1}(|g(x)|) \leq -\frac{c}{2}|x||g(x)|.$$

Notice that $|g|$ is increasing on $[0, \infty)$ and satisfies $\lim_{|x| \rightarrow \infty} |g(x)| = \infty$. Whence, there exists $M_0 > 0$ such that for every $r > 0$ and $|x| \geq 2r/c|g(M_0)| + M_0$,

$$\frac{x(G')^{-1}(g(x))}{|x|} \leq -\frac{c}{2}|g(x)| \leq -\frac{c}{2}|g(M_0)| \leq -\frac{r}{|x|}.$$

Thus, [48, Condition (6)] is satisfied and the results follows. For later use also note that, by [48, Lemma 1], we have the following uniform moment bounds:

$$\sup_{T \geq 0} \mathbb{E} \left[|X_T|^k \right] < \infty, \quad \text{for every } k \in \mathbb{N}. \quad (8.1)$$

□

Proof of Theorem 3.6. Market clearing evidently holds by definition of the trading rates (3.9). Observe that the corresponding positions φ^1 satisfy

$$\mu_t - \gamma^1 \sigma(\sigma \varphi_t^1 + \beta_t^1) = -\gamma \sigma^2 X_t. \quad (8.2)$$

Consider a competing admissible strategy ψ for agent 1. Identity (8.2) and the convexity of G yield

$$\begin{aligned} & J_T^1(\psi) - J_T^1(\dot{\varphi}^1) \\ &= \mathbb{E} \left[\int_0^T (\psi_t - \varphi_t^1) \mu_t - \frac{\gamma^1}{2} \sigma(\psi_t - \varphi_t^1) (\sigma \psi_t + \sigma \varphi_t^1 + 2\beta_t^1) + G(\dot{\varphi}_t^1) - G(\dot{\psi}_t) dt \right] \\ &= \mathbb{E} \left[\int_0^T (\psi_t - \varphi_t^1) \mu_t - \frac{\gamma^1}{2} \sigma(\psi_t - \varphi_t^1) (\sigma \psi_t - \sigma \varphi_t^1 + 2(\sigma \varphi_t^1 + \beta_t^1)) + G(\dot{\varphi}_t^1) - G(\dot{\psi}_t) dt \right] \\ &\leq \mathbb{E} \left[\int_0^T -\frac{1}{2} \gamma^1 \sigma^2 (\psi_t - \varphi_t^1)^2 + (\mu_t - \gamma^1 \sigma(\sigma \varphi_t^1 + \beta_t^1)) (\psi_t - \varphi_t^1) + G'(\dot{\varphi}_t^1) (\dot{\varphi}_t^1 - \dot{\psi}_t) dt \right] \\ &= \mathbb{E} \left[\int_0^T -\frac{1}{2} \gamma^1 \sigma^2 (\psi_t - \varphi_t^1)^2 - \gamma \sigma^2 X_t (\psi_t - \varphi_t^1) - G'(\dot{\varphi}_t^1) (\dot{\psi}_t - \dot{\varphi}_t^1) dt \right]. \end{aligned} \quad (8.3)$$

We now analyze the terms on the right-hand side. To ease notation, set

$$\dot{\theta}_t = \dot{\psi}_t - \dot{\varphi}_t^1, \quad \text{so that} \quad \theta_t = \int_0^t (\dot{\psi}_u - \dot{\varphi}_u^1) du = \psi_t - \varphi_t^1.$$

The dynamics (3.7) of X , Itô's formula, and the ODE (3.5) for g imply

$$\begin{aligned} dg(X_t) &= \left[\frac{1}{2} \delta^2 g''(X_t) + g'(X_t) (G')^{-1}(g(X_t)) \right] dt + \delta g'(X_t) dW_t \\ &= \gamma \sigma^2 X_t dt + \delta g'(X_t) dW_t. \end{aligned} \quad (8.4)$$

Integration by parts and the dynamics (8.4) in turn yield

$$d[\theta_t g(X_t)] = [\dot{\theta}_t g(X_t) + \gamma \sigma^2 X_t \theta_t] dt + \delta \theta_t g'(X_t) dW_t. \quad (8.5)$$

Here, the local martingale part is a true martingale. Indeed, by Hölder's inequality, the integrability condition (3.2) and the boundedness of g' established in Lemma A.5,

$$\mathbb{E} \left[\int_0^t |g'(X_u)|^2 \theta_u^2 du \right] \leq K^2 \mathbb{E} \left[\int_0^t \theta_u^2 du \right] < \infty.$$

Also taking into account that $G'(\dot{\varphi}_t^1) = G'(H(g(X_t))) = g(X_t)$, we can therefore use (8.5) to replace the second and the third terms on the right-hand side of (8.3), obtaining

$$J_T^1(\dot{\psi}) - J_T^1(\dot{\varphi}^1) \leq -\mathbb{E}[g(X_T)\theta_T] - \mathbb{E} \left[\int_0^T \frac{1}{2} \gamma^1 \sigma^2 \theta_t^2 dt \right].$$

The Cauchy-Schwartz inequality yields

$$|\mathbb{E}[g(X_T)\theta_T]| \leq \sqrt{\mathbb{E}[g(X_T)^2]\mathbb{E}[\theta_T^2]} \leq \sqrt{\mathbb{E}[2g(X_T)^2]}\sqrt{\mathbb{E}[(\psi_T)^2] + \mathbb{E}[(\varphi_T^1)^2]}.$$

By the polynomial growth of g established in Lemma A.5 and (8.1), we have $\sup_{T \geq 0} \mathbb{E}[g(X_T)^2] < \infty$. Together with the transversality condition (3.3), it follows that

$$0 \leq \lim_{T \rightarrow \infty} \frac{1}{T} |\mathbb{E}[g(X_T)\theta_T]| \leq \lim_{T \rightarrow \infty} \frac{1}{T} \sqrt{\mathbb{E}[2g(X_T)^2]}\sqrt{\mathbb{E}[(\psi_T)^2] + \mathbb{E}[(\varphi_T^1)^2]} = 0.$$

Therefore, the trading rate $\dot{\varphi}^1$ is indeed long-run optimal for agent 1:

$$\begin{aligned} \limsup_{T \rightarrow \infty} \frac{1}{T} \left[J_T^1(\dot{\psi}) - J_T^1(\dot{\varphi}^1) \right] &\leq \limsup_{T \rightarrow \infty} \frac{1}{T} \left[-\mathbb{E}[g(X_T)\theta_T] - \mathbb{E} \left[\int_0^T \frac{1}{2} \gamma^1 \sigma^2 \theta_t^2 dt \right] \right] \\ &= -\lim_{T \rightarrow \infty} \frac{1}{T} \mathbb{E}[g(X_T)\theta_T] + \limsup_{T \rightarrow \infty} \frac{1}{T} \mathbb{E} \left[-\int_0^T \frac{1}{2} \gamma^1 \sigma^2 \theta_t^2 dt \right] \leq 0. \end{aligned}$$

An analogous argument shows that $\dot{\varphi}^2$ is long-run optimal for agent 2. This completes the proof. \square

8.2 Proofs for Section 4

The following lemma provides the counterpart of the function g from Lemma 3.3 for proportional costs. It is given in closed form; its properties listed here are therefore easily verified by direct calculations:

Lemma 8.1. *With the constant l from (4.6), define*

$$g(x) = \frac{\gamma\sigma^2}{3\delta^2} (x^3 - 3l^2x) \mathbb{1}_{|x| \leq l} - \lambda \operatorname{sgn}(x) \mathbb{1}_{|x| > l}. \quad (8.6)$$

This function has the following properties:

- (i) g is an odd, decreasing function;
- (ii) $\frac{1}{2}\delta^2 g''(x) = \gamma\sigma^2 x$ for $x \in (-l, l)$;
- (iii) g' is continuous on \mathbb{R} and $g'(l) = g'(-l) = 0$;
- (iv) For every $x \in [0, l]$, we have $0 \geq g(x) \geq g(l) = -\lambda$.

Lemma 8.2. *The strategies from Theorem 4.2 are admissible and clear the market.*

Proof. Let $x = |\varphi_{0-}^1| + |\varphi_{0-}^2| + l + s$. First, note that the initial jump satisfies

$$-l \leq X_0 = L_0 - U_0 + X_{0-} \leq l,$$

and hence

$$X_t = \delta W_t + L_t - U_t + X_{0-}.$$

Therefore, we have

$$\mathbb{E}[|L_T - U_T|] = \mathbb{E}[|X_T - \delta W_T - X_{0-}|] \leq \delta \mathbb{E}[|W_T|] + \mathbb{E}[|X_T|] + |X_{0-}| \leq x + \delta \sqrt{\frac{2T}{\pi}},$$

so that the transversality condition (4.3) is satisfied.

Notice that

$$|L_t - U_t|^2 \leq (|X_t| + |X_{0-}| + \delta|W_t|)^2 \leq (x + \delta|W_t|)^2 \leq 2x^2 + 2\delta^2|W_t|^2.$$

As a consequence,

$$\mathbb{E} \left[\int_0^T (L_t - U_t)^2 dt \right] \leq \mathbb{E} \left[\int_0^T 2x^2 + 2\delta^2|W_t|^2 dt \right] = 2x^2T + 2\delta^2 \mathbb{E} \left[\int_0^T |W_t|^2 dt \right] = 2x^2T + \delta^2T^2,$$

so that φ^1 satisfies the first integrability condition in (4.2).

Now, apply Itô's formula to $(X_T + l)^2/4l$, obtaining

$$\begin{aligned} & \frac{1}{4l}(X_T + l)^2 - \frac{1}{4l}(X_0 + l)^2 \\ &= \int_0^T \frac{\delta}{2l}(X_t + l)dW_t + \int_0^T \frac{\delta^2}{4l}dt + \int_0^T \frac{1}{2l}(-l + l)dL_t - \int_0^T \frac{1}{2l}(l + l)dU_t \\ &= \int_0^T \frac{\delta}{2l}(X_t + l)dW_t + \frac{\delta^2}{4l}T - U_T + U_0. \end{aligned}$$

Rearranging, taking expectations, and taking into account that $0 \leq U_0 \leq |X_0| \leq x$ leads to

$$\begin{aligned} \mathbb{E}[U_T] &= U_0 + \frac{1}{4l}(X_0 + l)^2 + \frac{\delta^2}{4l}T - \mathbb{E} \left[\int_0^T \frac{\delta}{2l}(X_t + l)dW_t \right] - \mathbb{E} \left[\frac{1}{4l}(X_T + l)^2 \right] \\ &\leq x + l + \frac{\delta^2}{4l}T. \end{aligned} \tag{8.7}$$

After applying Itô's formula to $(X_T - l)^2/4l$, a symmetric calculation and $0 \leq L_0 \leq |X_0| \leq x$ show

$$\begin{aligned} \mathbb{E}[L_T] &= L_0 + \frac{1}{4l}(X_0 - l)^2 + \frac{\delta^2}{4l}T - \mathbb{E} \left[\int_0^T \frac{\delta}{2l}(X_t - l)dW_t \right] - \mathbb{E} \left[\frac{1}{4l}(X_T - l)^2 \right] \\ &\leq x + l + \frac{\delta^2}{4l}T. \end{aligned} \tag{8.8}$$

Combining (8.7) and (8.8) yields the second integrability condition in (4.2); therefore φ^1 is indeed admissible. Market clearing evidently holds by construction; in particular φ^2 is admissible as well. For later use also observe that, by definition,

$$\varphi_t^1 = X_t - \delta W_t + \frac{s\gamma^2}{\gamma^1 + \gamma^2}, \quad \gamma^1 \sigma(\sigma\varphi_t^1 + \beta_t^1) - \mu_t = \gamma\sigma^2 X_t. \tag{8.9}$$

□

Proof of Theorem 4.2. Consider a competing admissible strategy with Jordan-Hahn decomposition $\psi = \varphi_{0-}^1 + \psi^\uparrow - \psi^\downarrow$. To ease notation, set

$$\theta_t = \psi_t - \varphi_t^1, \quad \text{so that} \quad d\theta_t = d\psi_t^\uparrow - d\psi_t^\downarrow - dL_t + dU_t, \quad \theta_{0-} = 0.$$

By properties (i) and (iv) of g from Lemma 8.1, we have

$$\mathbb{1}_{(-l,0)}(X_t)g(X_t)d\theta_t \leq \lambda \mathbb{1}_{(-l,0)}(X_t) \left[d\psi_t^\uparrow + d\psi_t^\downarrow + dU_t \right], \quad (8.10)$$

$$\mathbb{1}_{(0,l)}(X_t)g(X_t)d\theta_t \leq \lambda \mathbb{1}_{(0,l)}(X_t) \left[d\psi_t^\uparrow + d\psi_t^\downarrow + dL_t \right]. \quad (8.11)$$

Since L, U only grow on the sets $\{X_t = -l\}$ and $\{X_t = l\}$, respectively, properties (i) and (iv) of g from Lemma 8.1 and (8.10-8.11) show that

$$\begin{aligned} & \int_{0-}^T g(X_t)d\theta_t \\ &= \lambda \int_{0-}^T \mathbb{1}_{\{-l\}}(X_t) \left[d\psi_t^\uparrow - d\psi_t^\downarrow - dL_t \right] - \mathbb{1}_{\{l\}}(X_t) \left[d\psi_t^\uparrow - d\psi_t^\downarrow + dU_t \right] + \mathbb{1}_{(-l,l)}(X_t)g(X_t)d\theta_t \\ &\leq \lambda \int_{0-}^T \mathbb{1}_{\{-l\}}(X_t) \left[d\psi_t^\uparrow - d\psi_t^\downarrow - dL_t \right] + \mathbb{1}_{\{l\}}(X_t) \left[d\psi_t^\downarrow - d\psi_t^\uparrow - dU_t \right] + \mathbb{1}_{(-l,l)}(X_t) \left[d\psi_t^\uparrow + d\psi_t^\downarrow \right] \\ &\leq \lambda \int_{0-}^T \mathbb{1}_{\{-l\}}(X_t) \left[d\psi_t^\uparrow + d\psi_t^\downarrow - dL_t \right] + \mathbb{1}_{\{l\}}(X_t) \left[d\psi_t^\uparrow + d\psi_t^\downarrow - dU_t \right] + \mathbb{1}_{(-l,l)}(X_t) \left[d\psi_t^\uparrow + d\psi_t^\downarrow \right] \\ &\leq \lambda \int_{0-}^T \left(\mathbb{1}_{\{-l\}}(X_t) + \mathbb{1}_{(-l,l)}(X_t) + \mathbb{1}_{\{l\}}(X_t) \right) \left[d\psi_t^\uparrow + d\psi_t^\downarrow - dL_t - dU_t \right] \\ &= \lambda \left[\psi_T^\uparrow + \psi_T^\downarrow - L_T - U_T \right] - \lambda \left[\psi_{0-}^\uparrow + \psi_{0-}^\downarrow - L_{0-} - U_{0-} \right] \\ &= \lambda \left[\psi_T^\uparrow + \psi_T^\downarrow - L_T - U_T \right]. \end{aligned}$$

Together with (8.9), it follows that

$$\begin{aligned} & J_T^1(\psi) - J_T^1(\varphi^1) \\ &= \mathbb{E} \left[\int_{0-}^T \left((\psi_t - \varphi_t^1)\mu_t - \frac{\gamma^1}{2}\sigma(\psi_t - \varphi_t^1)(\sigma\psi_t + \sigma\varphi_t^1 + 2\beta_t^1) \right) dt - \lambda(\psi_T^\uparrow + \psi_T^\downarrow) + \lambda(L_T + U_T) \right] \\ &= \mathbb{E} \left[\int_{0-}^T \left((\psi_t - \varphi_t^1)\mu_t - \frac{\gamma^1}{2}\sigma(\psi_t - \varphi_t^1)(\sigma\psi_t - \sigma\varphi_t^1 + 2(\sigma\varphi_t^1 + \beta_t^1)) \right) dt - \lambda(\psi_T^\uparrow + \psi_T^\downarrow - L_T - U_T) \right] \\ &= \mathbb{E} \left[\int_{0-}^T - \left(\frac{1}{2}\gamma^1\sigma^2(\psi_t - \varphi_t^1)^2 + \gamma\sigma^2X_t(\psi_t - \varphi_t^1) \right) dt - \lambda(\psi_T^\uparrow + \psi_T^\downarrow - L_T - U_T) \right] \\ &\leq -\mathbb{E} \left[\int_{0-}^T \frac{1}{2}\gamma^1\sigma^2\theta_t^2 dt \right] - \mathbb{E} \left[\int_{0-}^T \gamma\sigma^2X_t\theta_t dt + \int_{0-}^T g(X_t)d\theta_t \right]. \quad (8.12) \end{aligned}$$

To simplify this expression, use Itô's formula, the dynamics (4.5) of the doubly-reflected Brownian motion X , the growth properties of L and U , and the ODE for g from Lemma 8.1(ii) to compute

$$\begin{aligned} dg(X_t) &= \frac{1}{2}\delta^2g''(X_t)dt + g'(X_t)[dL_t - dU_t] + \delta g'(X_t)dW_t \\ &= \gamma\sigma^2X_tdt + \delta g'(X_t)dW_t. \end{aligned}$$

Integration by parts in turn yields

$$d[g(X_t)\theta_t] = g(X_t)d\theta_t + \gamma\sigma^2\theta_t X_t dt + \delta\theta_t g'(X_t)dW_t.$$

Since g' is bounded, the integrability condition (4.2) implies that the local martingale part in this decomposition is a true martingale, so that

$$\mathbb{E} \left[\int_{0-}^T \gamma\sigma^2 X_t \theta_t dt + \int_{0-}^T g(X_t) d\theta_t \right] = \mathbb{E}[g(X_T)\theta_T] - \mathbb{E}[g(X_{0-})\theta_{0-}] = \mathbb{E}[g(X_T)\theta_T]. \quad (8.13)$$

Now, the long-run optimality of φ^1 for agent 1 follows from (8.12) and (8.13) by taking into account that property (iv) of g and the transversality condition (4.3) imply

$$\lim_{T \rightarrow \infty} \frac{1}{T} |\mathbb{E}[g(X_T)\theta_T]| \leq \lim_{T \rightarrow \infty} \frac{1}{T} \mathbb{E}[|g(X_T)\theta_T|] \leq \lim_{T \rightarrow \infty} \frac{\lambda}{T} \mathbb{E}[|\theta_T|] \leq \lim_{T \rightarrow \infty} \frac{\lambda}{T} \mathbb{E}[|\psi_T| + |\varphi_T^1|] = 0.$$

An analogous argument shows that φ^2 is optimal for agent 2, thereby completing the proof. \square

A Proof of Lemma 3.3

In this appendix, we establish existence, uniqueness, and properties for the second order nonlinear ODE (3.5) from Lemma 3.3. To this end, we introduce the following first -order nonlinear ODE:

$$y'(x) = f(x, y(x)) := -ax^2 + b + F(y(x)), \quad (A.1)$$

and extend the ideas of [27] to general functions F which satisfy Assumption A.1. That is, in Lemma A.4, we establish that for suitable functions F , and any choice of $a > 0$ and $b \geq 0$, (A.1) has a unique positive solution on its maximal domain which contains $[\sqrt{b/a}, \infty)$. Then, for the first-order ODE:

$$g'(x) = ax^2 - b - F(g(x)), \quad (A.2)$$

Lemma A.5 shows that there is a unique value of b that guarantees there is a solution on \mathbb{R} such that $xg(x) \leq 0$, and the solution is unique. Moreover, Lemma A.6 proves that this solution to (A.2) is also the unique solution of the second-order ODE:

$$g''(x) = 2ax - F'(g(x))g'(x). \quad (A.3)$$

Finally, with the help of Lemma A.7 pointing out the relationship between Assumption 3.1 and Assumption A.1, we establish the proof of Lemma 3.3 with F chosen to be proportional to the Legendre transform of the trading cost function G .

To carry out this program, we first introduce the assumptions on F that are needed to generalize the argument developed for power functions by [27]. Subsequently, in Remark A.2 and Lemma A.3, we derive a number of consequences, which are crucial tools for the subsequent analysis.

Assumption A.1. (i) F is convex, differentiable, even, and strictly increasing on $[0, \infty)$ with $F(0) = 0$;

(ii) F' is also differentiable and strictly increasing on $[0, \infty)$ with $F'(0) = 0$;

(iii) There exists a constant K such that $F(x) \leq K(1 + |x|^p)$ for some $p \geq 2$;

(iv) There exist constants $\tilde{C} > 0$ and $x_0 > 0$ such that $F''(x) > \tilde{C}$ for every $|x| > x_0$.

Remark A.2. Some immediate consequences of Assumption A.1 are as follows:

- (i) F' is increasing on the whole real line, since it is an odd function (as F is even) and F' is strictly increasing on $[0, \infty)$;
- (ii) Assumption (iv) implies that there is some $\hat{a} > 0$ such that $F(x) > \hat{a}x^2$ for large $x > 0$. This is why $p \geq 2$ in Assumption A.1(iii) is without loss of generality.

Lemma A.3. *Suppose F satisfies Assumption A.1. Then:*

(i) F^{-1} exists and is concave on $[0, \infty)$;

(ii) For every $x \geq 0$ and every $\alpha \geq 1$:

$$\alpha F(x) \leq F(\alpha x), \quad F^{-1}(\alpha x) \leq \alpha F^{-1}(x);$$

(iii) For $x, y \geq 0$:

$$F(x+y) \geq F(x) + F(y), \quad F^{-1}(x) + F^{-1}(y) \geq F^{-1}(x+y);$$

(iv) On $(0, \infty)$, F^{-1} is strictly increasing but $(F^{-1})'$ is strictly decreasing;

(v) There exists constant $C > 0$ that $F^{-1}(x^2) \leq C|x|$ and $2x(F^{-1})'(x^2) \leq 2C$ for every $|x| > x_0$.

Proof. (i): Convexity of F implies that, for $x, y \geq 0$ and $0 < a < 1$,

$$ax + (1-a)y = aF(F^{-1}(x)) + (1-a)F(F^{-1}(y)) \geq F(aF^{-1}(x) + (1-a)F^{-1}(y)).$$

As F is increasing, F^{-1} is increasing as well. Applying F^{-1} on both sides of the above estimate in turn yields the concavity of F^{-1} .

(ii): Recall that $F(0) = 0$ and again use convexity of F to obtain, for every $x \geq 0$ and $\alpha \geq 1$,

$$F(\alpha x) = \alpha \left[\frac{1}{\alpha} F(\alpha x) + \left(1 - \frac{1}{\alpha}\right) F(0) \right] \geq \alpha F\left(\frac{1}{\alpha} \alpha x\right) = \alpha F(x).$$

Analogously, the concavity of F^{-1} yields $F^{-1}(\alpha x) \leq \alpha F^{-1}(x)$.

(iii): Since F' is increasing we have $F'(x+y) - F'(x) \geq 0$ for every $x, y > 0$. As a consequence, $F(x+y) - F(x) \geq F(0+y) - F(0) = F(y)$ as asserted. The same argument also yields the analogous estimate for F^{-1} .

(iv): Since F is convex and F and F' are strictly increasing on $[0, \infty)$, we have $F'(x) > 0$ and $F''(x) > 0$ for every $x > 0$,

$$(F^{-1})'(x) = \frac{1}{F'(F^{-1}(x))} > 0, \quad (F^{-1})''(x) = -\frac{F''(F^{-1}(x))}{(F'(F^{-1}(x)))^3} < 0$$

so that F^{-1} is strictly increasing on $[0, \infty)$ but $(F^{-1})'$ is strictly decreasing on $(0, \infty)$ as asserted.

(v): By directly integrating the inequality in Assumption A.1 (iv) and choosing C large enough, it's easy to see that the first statement holds. For the second statement, by Assumption A.1(ii),

$$\frac{d}{dx} [xF'(x) - F(x)] = xF''(x) + F'(x) - F'(x) = xF''(x) > 0, \quad \text{for } x > 0.$$

Hence,

$$F'(F^{-1}(x^2)) \geq \frac{F(F^{-1}(x^2))}{F^{-1}(x^2)} = \frac{x^2}{F^{-1}(x^2)}.$$

Together Assumption A.1(iv) it follows that, for $x \geq |x_0|$,

$$\frac{d}{dx}F^{-1}(x^2) = 2x(F^{-1})'(x^2) = \frac{2x}{F'(F^{-1}(x^2))} \leq \frac{2xF^{-1}(x^2)}{x^2} \leq \frac{2Cx^2}{x^2} = 2C,$$

which yields the desired result. \square

Now we address the existence and uniqueness of the positive solution to (A.1) on $[\sqrt{b/a}, \infty)$.

Lemma A.4. *Let F be a function satisfying Assumption A.1 and $a > 0$, $b \geq 0$. Then there exists a unique solution y of*

$$y'(x) = f(x, y(x)) := -ax^2 + b + F(y(x)), \quad (\text{A.1})$$

such that $[0, \infty)$ is contained in its maximal interval of existence, and $y(x) \geq 0$ for every $x \geq \sqrt{b/a}$. Moreover, y is increasing on $[\sqrt{b/a}, \infty)$ and satisfies the growth condition

$$\lim_{x \rightarrow \infty} \frac{y(x)}{F^{-1}(ax^2)} = 1. \quad (\text{A.4})$$

Further, in (A.1), if we consider $y(x) = y(x; b)$, then on $[0, \infty)$,

$$\frac{\partial y(x; b)}{\partial b} < 0. \quad (\text{A.5})$$

Proof. On $[\sqrt{b/a}, +\infty)$, define the function $h(x) := F^{-1}(ax^2 - b)$. Notice that by definition of $h(x)$ we have $f(x, h(x)) = 0$ and h is strictly increasing on $[\sqrt{b/a}, +\infty)$. Thus we can infer that h is a supersolution on $(\sqrt{b/a}, \infty)$ in that $h'(x) \geq f(x, h(x))$.

Notice that $f(x, y)$ is locally Lipschitz, so that local existence and uniqueness hold for the initial-value problem (A.1). For every $\bar{x} \in [\sqrt{b/a}, +\infty)$, let $y(x; \bar{x}, h(\bar{x}))$ denote the unique solution to (A.1) with initial condition $(\bar{x}, h(\bar{x}))$ on its maximal interval of existence. By directly calculating the first-order derivative, we find that for every $\bar{x} > \sqrt{b/a}$,

$$y'(\bar{x}; \bar{x}, h(\bar{x})) = -a\bar{x}^2 + b + F(y(\bar{x}; \bar{x}, h(\bar{x}))) = -a\bar{x}^2 + b + F(h(\bar{x})) = 0.$$

For the second-order derivative, we observe

$$y''(x; \bar{x}, h(\bar{x})) = -2ax + F'(y(x; \bar{x}, h(\bar{x})))y'(x; \bar{x}, h(\bar{x})),$$

which implies that $y''(\bar{x}; \bar{x}, h(\bar{x})) < 0$ and $y'(x; \bar{x}, h(\bar{x})) < 0$, where $x \in (\bar{x}, \bar{x} + \epsilon)$ for some $\epsilon > 0$. In addition, for every $x > \bar{x}$ such that $y(x; \bar{x}, h(\bar{x})) \geq 0$ still holds, we have $F'(y(x; \bar{x}, h(\bar{x}))) \geq 0$ and thus also $y''(x; \bar{x}, h(\bar{x})) < 0$, and $y'(x; \bar{x}, h(\bar{x})) < 0$. This means that y will keep decreasing until it is finally below 0, from which we can further infer that for $x > \bar{x}$, $y(x; \bar{x}, h(\bar{x})) \leq h(x)$. On the other hand, for $x \in [\sqrt{b/a}, \bar{x})$ in the maximal interval of existence, we can apply a symmetric argument where we let $x < \bar{x}$ go backwards. This shows $y(x; \bar{x}, h(\bar{x})) \geq h(x) \geq 0$ and, since

$$y'(x; \bar{x}, h(\bar{x})) = -ax^2 + b + F(y(x; \bar{x}, h(\bar{x}))) \geq -ax^2 + b + F(h(x)) = 0,$$

$y(x; \bar{x}, h(\bar{x}))$ is increasing on $[\sqrt{b/a}, \bar{x})$. Moreover, a comparison argument shows that for every $\bar{x} > \sqrt{b/a}$, $[\sqrt{b/a}, \bar{x}]$ is contained in the maximal interval of existence of $y(x; \bar{x}, h(\bar{x}))$. And for

$\bar{x}_1 < \bar{x}_2$, by the fact that the graph of the solutions cannot cross due to the local uniqueness, and the fact that $y(x; \bar{x}_1, h(\bar{x}_1))$ is decreasing at \bar{x}_1 while $y(x; \bar{x}_2, h(\bar{x}_2))$ is increasing, the graph of $y(x; \bar{x}_1, h(\bar{x}_1))$ lies below the graph of $y(x; \bar{x}_2, h(\bar{x}_2))$.

Next, we show that any solution y of (A.1) such that $[\sqrt{b/a}, \infty)$ is contained in its maximum interval of existence, and $y(x) \geq 0$ for every $x \geq \sqrt{b/a}$, automatically satisfies the growth condition (A.4). From the above argument concerning the relationship between $h(x)$ and $y(x; \bar{x}, h(\bar{x}))$, an important observation is that for every $x \in [\sqrt{b/a}, \infty)$, we need to have $y(x) > h(x)$, otherwise the solution will not stay positive. We summarize the properties of y as follows:

- i) $y(x) > h(x) \geq 0$, and $y'(x) = -ax^2 + b + F(y(x)) > -ax^2 + b + F(h(x)) = 0$, which means y is strictly increasing on $[\sqrt{b/a}, +\infty)$;
- ii) $[\sqrt{b/a}, +\infty) \subset D$, where D is the maximal interval of existence of $y(x)$.

From property i) and Lemma A.3(iii,iv), it follows that

$$1 = \lim_{x \rightarrow \infty} \frac{F^{-1}(ax^2) - F^{-1}(b)}{F^{-1}(ax^2)} \leq \liminf_{x \rightarrow \infty} \frac{h(x)}{F^{-1}(ax^2)} \leq \limsup_{x \rightarrow \infty} \frac{h(x)}{F^{-1}(ax^2)} \leq \lim_{x \rightarrow \infty} \frac{F^{-1}(ax^2)}{F^{-1}(ax^2)} = 1,$$

and in turn

$$\liminf_{x \rightarrow \infty} \frac{y(x)}{F^{-1}(ax^2)} \geq 1.$$

Next we show that $L := \lim_{x \rightarrow \infty} \frac{y(x)}{F^{-1}(ax^2)}$ exists and $L = 1$. To this end, set $M := \limsup_{x \rightarrow \infty} \frac{y(x)}{F^{-1}(ax^2)}$ and notice that $1 \leq M \leq \infty$. If $M = 1$ then we can conclude $L = 1$.

Assume $1 < M < \infty$. We first want to show $M = L$. Then there is a sequence $(x_n)_{n \geq 0} \rightarrow \infty$ such that $\lim_{n \rightarrow \infty} \frac{y(x_n)}{F^{-1}(ax_n^2)} = M$. In particular, for any $\delta \in (0, M - 1)$ there exists $N_\delta \in \mathbb{N}$ such that for every $n \geq N_\delta$ we have

$$y(x_n) \geq (M - \delta)F^{-1}(ax_n^2).$$

For large x , we claim that the function $s(x) = (M - \delta)F^{-1}(ax^2)$ is a subsolution of (A.1). By Lemma A.3(v), we know that for $x \geq |x_0|/\sqrt{a}$,

$$0 < s'(x) = (M - \delta)(F^{-1})'(ax^2)2ax \leq 2\sqrt{a}(M - \delta)C.$$

Since $M - \delta > 1$, there exists \bar{x} such that for $x \geq \bar{x}$, we have $(M - \delta)ax^2 - ax^2 + b \geq 2\sqrt{a}(M - \delta)C$. As a consequence,

$$\begin{aligned} s'(x) &\leq 2\sqrt{a}(M - \delta)C \leq -ax^2 + b + (M - \delta)ax^2 \\ &= -ax^2 + b + F(F^{-1}((M - \delta)ax^2)) \\ &\leq -ax^2 + b + F((M - \delta)F^{-1}(ax^2)) = f(x, s(x)). \end{aligned}$$

Thus, for every $\delta \in (0, M - 1)$ and some \bar{x} , we have $y(x) \geq s(x) = (M - \delta)F^{-1}(ax^2)$ for $x \geq \bar{x}$. In particular, for every small δ ,

$$\liminf_{x \rightarrow \infty} \frac{y(x)}{F^{-1}(ax^2)} \geq M - \delta,$$

and therefore

$$\liminf_{x \rightarrow \infty} \frac{y(x)}{F^{-1}(ax^2)} = M = \limsup_{x \rightarrow \infty} \frac{y(x)}{F^{-1}(ax^2)}.$$

If $M = \infty$, we substitute $M - \delta$ with $N \in \mathbb{N}$ and then infer with the same argument that $\liminf_{x \rightarrow \infty} \frac{y(x)}{F^{-1}(ax^2)} = \infty$. In other words, the limit L exists and $L = M \in (1, \infty]$.

Next, we show $L = 1$. First, assume to the contrary $1 < L < \infty$. Since $\lim_{x \rightarrow \infty} \frac{y(x)}{F^{-1}(ax^2)} = L$, and by Assumption A.1(iv), there exists a constant $K > 0$ such that $y(x) \leq Kx$ for large $x > 0$. Moreover, for every $\delta \in (0, L - 1)$ and large x , by Property A.3(ii),

$$y(x) \geq (L - \delta)F^{-1}(ax^2) \geq F^{-1}((L - \delta)ax^2).$$

As a consequence,

$$\liminf_{x \rightarrow \infty} \frac{F(y(x))}{ax^2} \geq L - \delta.$$

On the other hand, (A.1) implies

$$\liminf_{x \rightarrow \infty} \frac{y'(x)}{ax^2} = L - \delta - 1 > 0,$$

so that $y'(x)$ grows at least quadratically, leading to a contradiction.

Now assume that $L = +\infty$. From (A.1) it follows that

$$\lim_{x \rightarrow \infty} \frac{y'(x)}{F(y(x))} = 1.$$

Notice that for large x such that $y(x) > Cx_0$, Assumption A.1(iv) yields

$$\frac{y(x)^2}{C^2} = F\left(F^{-1}\left(\frac{y(x)^2}{C^2}\right)\right) \leq F\left(C\frac{y(x)}{C}\right) = F(y(x)).$$

Thus, for small δ and sufficiently large x , we have $\frac{1-\delta}{C^2}y^2(x) \leq (1-\delta)F(y(x)) \leq y'(x)$. This implies that, for large $x > \bar{x}$,

$$y(x) \geq \frac{1}{\frac{1}{y(\bar{x})} - \frac{1-\delta}{C^2}(x - \bar{x})}.$$

In particular, $y(x)$ has a vertical asymptote, contradicting Property ii). In summary, we therefore have $L = 1$.

We now show the uniqueness of $y(x)$. Suppose there exists another solution y_2 of (A.1) such that $[\sqrt{b/a}, \infty)$ is contained in its maximal domain, and $y_2(x) \geq 0$ for every $x \geq \sqrt{b/a}$, and there exists \bar{x} , $\delta > 0$ such that $y_2(\bar{x}) \geq y(\bar{x}) + \delta$. Then, on $[\bar{x}, \infty)$, the graph of y_2 always lies above y otherwise it will violate the local uniqueness of (A.1). Moreover, for $x \geq \bar{x}$,

$$y_2'(x) - y'(x) = F(y_2(x)) - F(y(x)) \geq 0,$$

which means $y_2 - y$ is increasing. As a result,

$$y_2'(x) - y'(x) = F(y_2(x)) - F(y(x)) \geq F(y_2(x) - y(x)) \geq F(y_2(\bar{x}) - y(\bar{x})) \geq F(\delta) > 0,$$

which implies that, for every $x > \bar{x}$,

$$y_2(x) - y(x) \geq \delta + (x - \bar{x})F(\delta).$$

But then, since y_2 also satisfies (A.4), and for large x we have $F^{-1}(ax^2) \leq \sqrt{a}Cx$,

$$0 = \lim_{x \rightarrow \infty} \frac{y_2(x) - y(x)}{F^{-1}(ax^2)} \geq \lim_{x \rightarrow \infty} \frac{\delta + (x - \bar{x})F(\delta)}{\sqrt{a}Cx} = \frac{F(\delta)}{\sqrt{a}C} > 0,$$

leads to contradiction. A symmetric argument yields the same results for the case where there exists \bar{x} and $\delta > 0$ such that $y_2(\bar{x}) \leq y(\bar{x}) - \delta$. This establishes uniqueness.

We now establish existence of a solution with the asserted properties. To this end, define $y_*(x) := \sup\{y(x; \bar{x}, h(\bar{x})) : \bar{x} \in [\sqrt{b/a}, +\infty)\}$ for every x in the union of the maximal existence of interval of $y(x; \bar{x}, h(\bar{x}))$.

By Lemma A.3(v), for every $x_1 \geq 0$, we can choose a large $y_1 > F^{-1}(ax_1^2 + 2\sqrt{a}C + x_0)$ such that the function $\tilde{y}(x) = F^{-1}(F(y_1) + a(x^2 - x_1^2))$ is a subsolution to (A.1): choose y_1 large enough such that

$$\tilde{y}'(x) = 2ax(F^{-1})'(F(y_1) + a(x^2 - x_1^2)) \leq 2\sqrt{a}C \leq F(y_1) - ax_1^2 + b = f(x, \tilde{y}(x)).$$

Moreover, again by the fact the subsolution and the supersolution cannot cross, the graph of \tilde{y} does not intersect the graph of h on $[\sqrt{b/a}, \infty)$. In particular, the unique local solution $y(x; x_1, y_1)$ to (A.1) with initial condition (x_1, y_1) satisfies

$$\tilde{y}'(x_1) \leq f(x_1, \tilde{y}(x_1)) = f(x_1, y_1) = y'(x_1; x_1, y_1).$$

A comparison argument shows that $[\sqrt{b/a}, \infty)$ is contained in the maximal interval of existence of $y(x; x_1, y_1)$, hence is strictly larger than $h(x)$ for every $x \geq \sqrt{b/a}$. Thus for every $\bar{x} \geq \sqrt{b/a}$, the graph of $y(x; x_1, y_1)$ lies above $y(x; \bar{x}, h(\bar{x}))$ and, in particular, $y_1 = y(x_1; x_1, y_1) > y(x_1; \bar{x}, h(\bar{x}))$. Taking the supremum over \bar{x} yields that $y_*(x_1) \leq y_1 < +\infty$.

Moreover, for every $x \geq \sqrt{b/a}$ and every $\epsilon > 0$,

$$\begin{aligned} y_*(x + \epsilon) - y_*(x) &= \sup\{y(x + \epsilon; \bar{x}, h(\bar{x})) - y_*(x) : \bar{x} \in [\sqrt{b/a}, +\infty)\} \\ &\leq \sup\{y(x + \epsilon; \bar{x}, h(\bar{x})) - y(x; \bar{x}, h(\bar{x})) : \bar{x} \in [\sqrt{b/a}, +\infty)\} \\ &\leq \int_x^{x+\epsilon} \sup\{y'(\xi; \bar{x}, h(\bar{x})) : \bar{x} \in [\sqrt{b/a}, +\infty)\} d\xi \\ &= \int_x^{x+\epsilon} -a\xi^2 + b + \sup\{F(y(\xi; \bar{x}, h(\bar{x}))) : \bar{x} \in [\sqrt{b/a}, +\infty)\} d\xi \\ &= \int_x^{x+\epsilon} -a\xi^2 + b + F(y_*(\xi)) d\xi \\ &= \int_x^{x+\epsilon} f(\xi, y_*(\xi)) d\xi. \end{aligned}$$

As a consequence,

$$\limsup_{\epsilon \rightarrow 0} \frac{y_*(x + \epsilon) - y_*(x)}{\epsilon} \leq f(x, y_*(x)).$$

On the other hand, notice that for arbitrary $\bar{x} > x > \sqrt{b/a}$, $y(x; \bar{x}, h(\bar{x}))$ is increasing in \bar{x} , thus for every $\epsilon, \delta > 0$ there exists $\bar{x} > x + \epsilon$ such that $y(x; \bar{x}, h(\bar{x})) + \delta > y_*(x)$. In this case, $y(\xi; \bar{x}, h(\bar{x}))$ is still increasing in the interval $[x, x + \epsilon]$, and for every $\xi \in [x, x + \epsilon]$,

$$F(y(\xi; \bar{x}, h(\bar{x}))) \geq F(y(x; \bar{x}, h(\bar{x}))) \geq F(y_*(x) - \delta).$$

Therefore,

$$\begin{aligned}
y_*(x + \epsilon) - y_*(x) &\geq -\delta + y_*(x + \epsilon) - y(x; \bar{x}, h(\bar{x})) \\
&\geq y(x + \epsilon; \bar{x}, h(\bar{x})) - y(x; \bar{x}, h(\bar{x})) - \delta \\
&= \int_x^{x+\epsilon} y'(\xi; \bar{x}, h(\bar{x})) d\xi - \delta \\
&= \int_x^{x+\epsilon} (-a\xi^2 + b + F(y(\xi; \bar{x}, h(\bar{x}))) d\xi - \delta \\
&\geq \epsilon F(y_*(x) - \delta) - \delta + \int_x^{x+\epsilon} (-a\xi^2 + b) d\xi.
\end{aligned}$$

As this holds for arbitrary small $\delta > 0$, it follows that

$$y_*(x + \epsilon) - y_*(x) \geq \epsilon F(y_*(x)) + \int_x^{x+\epsilon} (-a\xi^2 + b) d\xi,$$

and in turn

$$\liminf_{\epsilon \rightarrow 0} \frac{y_*(x + \epsilon) - y_*(x)}{\epsilon} \geq -ax^2 + b + F(y_*(x)) = f(x, y_*(x)).$$

In summary, y_* therefore is a solution to (A.1) and satisfies properties i), ii) and hence satisfies also the growth condition (A.4).

Finally, for $b_2 > b_1 \geq 0$, we show the relationship between y_1 and y_2 . Define as before $h_1(x) = F^{-1}(ax^2 - b_1)$ and $h_2(x) = F^{-1}(ax^2 - b_2)$. Observe that $h_1(\bar{x}) > h_2(\bar{x})$ for $\bar{x} > \sqrt{b_2/a}$ and because note that any solution of (A.1) with coefficient b_1 is a subsolution of (A.1) with coefficient b_2 . Whence, a comparison argument shows that the unique local solution $y_1(x; \bar{x}, h_1(\bar{x}))$ of the first equation with initial condition $(\bar{x}, h_1(\bar{x}))$ lies above the unique local solution $y_2(x; \bar{x}, h_2(\bar{x}))$ of the second equation with terminal condition $(\bar{x}, h_2(\bar{x}))$. Another comparison argument guarantees that $y_1(x; \bar{x}, h_1(\bar{x}))$ and $y_2(x; \bar{x}, h_2(\bar{x}))$ cannot cross. Therefore, it follows that $[\sqrt{b_1/a}, \infty)$ is contained in both of the maximal interval of existence of y_1 and y_2 with $y_1(x) \geq y_2(x)$.

Now, we show that $y_1 > y_2$ on $[\sqrt{b_1/a}, \infty)$. Suppose to the contrary that there exists $x_0 \geq \sqrt{b_1/a}$ such that $y_1(x_0) = y_2(x_0)$. Then,

$$y_1'(x_0) = -ax_0^2 + b_1 + F(y_1(x_0)) = -ax_0^2 + b_1 + F(y_2(x_0)) < -ax_0^2 + b_2 + F(y_2(x_0)) = y_2'(x_0),$$

which means that there exists $\epsilon > 0$ such that for $x \in (x_0, x_0 + \epsilon)$, $y_2(x) > y_1(x)$. This contradicts that $y_1(x) \geq y_2(x)$ on $[\sqrt{b_1/a}, \infty)$. Hence we conclude $y_1(x) > y_2(x)$. By a standard argument [15, Proposition 2.76, Theorem 2.77], $y(x; b)$ is differentiable with respect to b , and for every $b > 0$, $[0, \sqrt{b/a}]$ is also contained in the maximal interval of existence of $y(x; b)$. Hence we can infer (A.5) holds, and $[0, \infty)$ is contained in the maximal interval of existence of y for every $b \geq 0$. \square

In A.4, we have shown that every $b \geq 0$, there exists non-negative solution y_r to (A.1) on $[0, \infty)$. A symmetric argument yields that for every $b \geq 0$, there exists a non-positive solution y_l to (A.1) on $(-\infty, 0]$. Then by the monotonicity of $y(0; b)$ with respect to b , there exists a unique choice of the constant b in (A.1) that allows to smoothly paste together the solution y_l and y_r at 0, thereby obtaining a solution of (A.1) on the whole real line which satisfies $xg(x) \leq 0$ for every $x \in \mathbb{R}$.

Lemma A.5. *Let F be a function satisfying Assumption A.1. Then there exists a unique constant b_F such that the ODE*

$$g'(x) = ax^2 - b - F(g(x)), \tag{A.2}$$

has a solution g on \mathbb{R} such that $xg(x) \leq 0$. Moreover, g is unique, and it is odd and decreasing and satisfies the following growth conditions:

$$\lim_{x \rightarrow -\infty} \frac{g(x)}{F^{-1}(ax^2)} = 1, \quad \lim_{x \rightarrow +\infty} \frac{g(x)}{F^{-1}(ax^2)} = -1. \quad (\text{A.6})$$

Further, there exists $K > 0$, such that

$$|g(x)| \leq K(1 + |x|), \quad |g'(x)| \leq K.$$

Proof. From Lemma A.4, we know that for every parameter $b \geq 0$ there exists a unique solution $y_r(x; b)$ on its maximal domain D_b of existence and $y_r(x; b) \geq 0$ for every $x \geq \sqrt{b/a}$, and $y_r(x; b)$ is unique and satisfies

$$\lim_{x \rightarrow +\infty} \frac{y_r(x; b)}{F^{-1}(ax^2)} = 1.$$

By Lemma A.4, we have $[0, \infty) \subset D_b$. Define $y_l(x; b) = -y_r(-x; b)$ on $(-\infty, 0]$, then

$$\lim_{x \rightarrow -\infty} \frac{y_l(x; b)}{F^{-1}(ax^2)} = - \lim_{x \rightarrow -\infty} \frac{y_r(-x; b)}{F^{-1}(ax^2)} = - \lim_{x \rightarrow \infty} \frac{y_r(x; b)}{F^{-1}(ax^2)} = -1.$$

Moreover, since F is even, for $x \leq 0$,

$$\begin{aligned} y_l'(x; b) &= y_r'(-x; b) = -a(-x)^2 + b + F(y_r(-x; b)) = -ax^2 + b + F(-y_r(-x; b)) \\ &= -ax^2 + b + F(y_l(x; b)). \end{aligned} \quad (\text{A.7})$$

That is, $y_l(x; b)$ also satisfies (A.1) on $(-\infty, 0]$.

For $b = 0$, by i) in the proof of Lemma A.4, $y_r(x; 0) > F^{-1}(ax^2)$, hence

$$y_r(0; 0) > F^{-1}(0) = 0 > -y_r(0; 0) = y_l(0; 0).$$

By (A.5) in Lemma A.4, for $x \geq 0$, $y_r(x; b)$ is strictly decreasing in b and $y_r(x; b) \leq y_r(x; 0) < \infty$. In addition, we claim that as $b \rightarrow +\infty$, $y_r(0; b)$ goes to $-\infty$. Suppose not, then there exists $\delta_1 := \lim_{b \rightarrow +\infty} y_r(0; b) > -\infty$. As a result,

$$y_r(1; b) = y_r(0; b) + \int_0^1 -ax^2 + b + F(y_r(x; b)) \, dx \geq y_r(0; b) + \int_0^1 (-a + b) \, dx \geq \delta_1 + b - a,$$

and, for $b \rightarrow +\infty$,

$$y_r(1; 0) \geq \limsup_{b \rightarrow +\infty} y_r(1; b) \geq \liminf_{b \rightarrow +\infty} y_r(1; b) \geq \lim_{b \rightarrow +\infty} \delta_1 + b - a = +\infty,$$

which leads to contradiction. Hence as $b \rightarrow +\infty$, $y_r(0; b)$ goes to $-\infty$, and $y_l(0; b) = -y_r(0; b)$ goes to $+\infty$. Thus, for some constant b_F we have 0 is contained in D_{b_F} and

$$y_r(0; b_F) = 0 = y_l(0; b_F). \quad (\text{A.8})$$

As $y_r(x; b)$ is decreasing in b , the constant b_F is unique.

Now we use $y_r(\cdot; b_F)$ and $y_l(\cdot; b_F)$ to construct the solution for (A.2):

$$g(x) := -y_r(x; b_F) \mathbb{1}_{[x \geq 0]} - y_l(x; b_F) \mathbb{1}_{[x < 0]}.$$

It's easy to see that g is defined on \mathbb{R} and satisfies the growth conditions (A.6). We now show that g is indeed a solution of (A.2). Using (A.8), we can see that g is continuous at $x = 0$. Therefore,

$$g(x) = -y_r(x; b_F) \mathbb{1}_{[x \geq 0]} + y_r(-x; b_F) \mathbb{1}_{[x < 0]} = -y_r(x; b_F) \mathbb{1}_{[x > 0]} + y_r(-x; b_F) \mathbb{1}_{[x \leq 0]} = -g(-x),$$

which implies that g is odd. Furthermore, as y_r is increasing on $[\sqrt{b_F/a}, \infty)$, and for $x \in [0, \sqrt{b_F/a}]$,

$$y_r'(x; b_F) = -ax^2 + b_F + F(y_r(x; b_F)) \geq -ax^2 + b_F \geq 0,$$

hence y_r is increasing on $[0, \infty)$, and we infer that g is decreasing. Since F is even, we have

$$F(g(x)) = F(-y_r(x; b_F)) = F(-y_l(-x; b_F)) = F(g(-x)), \quad \text{for } x \geq 0.$$

Therefore we can conclude that

$$g'(x) = -y_r'(x) = ax^2 - b_F - F(y_r(x; b_F)) = ax^2 - b_F - F(g(x)), \quad \text{for } x > 0.$$

Likewise,

$$g'(x) = -y_l'(x) = ax^2 - b_F - F(y_l(x; b_F)) = ax^2 - b_F - F(g(x)), \quad \text{for } x < 0.$$

Moreover, the continuity of g' is guaranteed at $x = 0$ since

$$\lim_{x \rightarrow 0^+} g'(x; b_F) = -y_r'(0; b_F) = -b_F = -y_l'(0; b_F) = \lim_{x \rightarrow 0^-} g'(x; b_F).$$

In summary, g therefore is indeed a solution of (A.2) with $b = b_F$.

Next, we show that g is unique. With $b = b_F$, we know from Lemma A.4 that there is a unique solution $y_r(x; b_F)$ of (A.1) with maximal domain D_{b_F} containing $[0, \infty)$. Moreover, notice that $y_l(x; b_F)$ also satisfies (A.1) with $b = b_F$, which implies that $D_{b_F} = \mathbb{R}$. Hence for every $x < 0$, we have $y_l(x; b_F) = y_r(x; b_F)$ and in turn $g(x) = -y_r(x; b_F)$ for $x \in \mathbb{R}$. The uniqueness of g follows from the uniqueness of $y_r(\cdot; b_F)$ for the unique choice of b_F .

The growth condition (A.6) implies that there exist $x_0 > 0$ and $\hat{c} > 0$ such that, for every $|x| > x_0$,

$$|g(x)| = |y_r(|x|)| \leq 2|F^{-1}(ax^2)| \leq 2\hat{c}|x|.$$

Therefore, for all x , and since $-g$ is increasing,

$$|g(x)| \leq \sup_{[-x_0, x_0]} |g(x)| + 2c|x| \leq |g(x_0)| + 2\hat{c}|x|. \quad (\text{A.9})$$

Now we would like to show the boundedness of g' , which follows the same idea as [8]. Since g is odd, we only need to show that for $x > 0$, g' is bounded from below. From (A.9), we can infer that as $x \rightarrow \infty$, g' cannot go to $-\infty$. Therefore, there exists $M > 0$ and an increasing sequence $\{x_n\}_{n=1}^\infty$ such that $x_n \rightarrow \infty$ and $-M \leq g'(x_n) \leq 0$. Now suppose g' is not bounded from below, which means that for every integer $n > M$, there exists $z_n > x_n$ such that $g'(z_n) \leq -n$. For each $n > M$, let $m(n) > n$ denote the first integer such that $x_n < z_n < x_{m(n)}$. Then from

$$g'(z_n) \leq -n < -M \leq \min\{g'(x_n), g'(x_{m(n)})\},$$

we can infer that there exists a local minimum of g' on $[x_n, x_{m(n)}]$ for every integer $n > M$, denoted by ξ_n . Therefore, for every integer $n > M$, $g''(\xi_n) = 0$, and

$$0 \leq g'''(\xi_n) = 2a - F''(g(\xi_n))(g'(\xi_n))^2 - F'(g(\xi_n))g''(\xi_n) = 2a - F''(g(\xi_n))(g'(\xi_n))^2.$$

Together with Assumption A.1 (ii, iv), we know that $F''(g(\xi_n)) > 0$, and hence for n large enough

$$n^2 \leq (g'(\xi_n))^2 \leq \frac{2a}{F''(g(\xi_n))} \leq \frac{2a}{\bar{C}},$$

which leads to a contradiction. Without loss of generality, we choose $M > 0$ large enough so that $|g'(x)| < M$ for every $|x| > x_0$.

Now choose $K > M + |g(x_0)| + 2\hat{c}$, we have

$$|g(x)| \leq K(1 + |x|), \quad |g'(x)| \leq K$$

as asserted. This completes the proof. \square

Next, we show that with $b = b_F$, the solution to the first-order ODE (A.2) on \mathbb{R} with $xg(x) \leq 0$ is also the unique solution on \mathbb{R} to the second-order ODE (A.3) with $xg(x) \leq 0$.

Lemma A.6. *Let F be a function satisfying Assumption (A.1). Then the unique solution g on \mathbb{R} to (A.2) such that $xg(x) \leq 0$ is also the unique solution on \mathbb{R} of the second-order ODE*

$$g''(x) = 2ax - F'(g(x))g'(x) \tag{A.3}$$

such that $xg(x) \leq 0$.

Proof. In view of the first-order ODE (A.2) satisfied by g , its derivative is also differentiable. Differentiating the ODE for g in turn shows that g also satisfies the second-order ODE (A.3).

Now suppose \tilde{g} is a solution of the second-order ODE (A.3) with $xg(x) \leq 0$. As

$$[F(\tilde{g}(x))]'' = F'(\tilde{g}(x))\tilde{g}'(x),$$

integrating both sides of (A.3) gives

$$\tilde{g}'(x) = \tilde{g}'(0) + \int_0^x (2a\xi - F'(\tilde{g}(\xi))\tilde{g}'(\xi))d\xi = ax^2 - \tilde{b} - F(\tilde{g}(x)),$$

for some constant \tilde{b} . By Lemma A.5 we know that b_F is the unique constant such that (A.2) has a solution on \mathbb{R} with $xg(x) \leq 0$. Thus, $\tilde{b} = b_F$ and, by the uniqueness of g , we have $\tilde{g} = g$. This completes the proof. \square

We introduce one more Lemma before the proof of Lemma 3.3

Lemma A.7. *Suppose the general cost function G satisfies Assumption 3.1. Then G^* , the Legendre transform of G , satisfies Assumption A.1, and so does cG^* , where $c > 0$ is a constant.*

Proof. Observe that the Legendre transformation of the cost function $G(x)$ is

$$G^*(x) = x(G')^{-1}(x) - G((G')^{-1}(x)).$$

Since the instantaneous cost G is even, G' and in turn $(G')^{-1}$ are odd, so that the function G^* is even. Moreover, $G(0) = G'(0) = 0$ imply $G^*(0) = 0$. As both G and $(G')^{-1}$ are differentiable,

$$(G^*)'(x) = (G')^{-1}(x) > 0.$$

In particular, $(G^*)^{-1}$ exists on $[0, \infty)$ and is differentiable. Moreover, by the convexity and twice differentiability of G ,

$$(G^*)''(x) = ((G')^{-1})'(x) > 0.$$

It follows that G^* is convex and $(G^*)'$ is strictly increasing, so that Assumptions A.1 (i,ii) are satisfied. By Assumption 3.1, $|((G')^{-1})'(x)| \leq C(1 + |x|^{k-1})$ for $C > 0$ and $k \geq 2$. Whence, there exists a constant $K > 0$ such that

$$G^*(x) = |G^*(x)| \leq |x(G')^{-1}(x)| \leq C(|x| + |x|^k) \leq K(1 + |x|^k).$$

Therefore, Assumption A.1(iii) is also satisfied. Again by Assumption 3.1, there exists $C > 0$ and $x_0 > 0$, such that for large $x > x_0$, $((G')^{-1})'(x) \geq \frac{1}{C}$, and hence

$$(G^*)''(x) = ((G')^{-1})'(x) \geq \frac{1}{C}.$$

Thus, Assumption A.1(iv) holds as well. \square

We now turn to the proof of Lemma 3.3.

Proof of Lemma 3.3. Let G^* denote the Legendre transform of G , and define

$$a = \frac{\gamma\sigma^2}{\delta^2}, \quad F(x) = \frac{2}{\delta^2}G^*(x),$$

where γ and δ are defined as in Lemma 3.3. By Lemma A.7, G^* and in turn F satisfy Assumption A.1. For the above choices of a and F , Lemma A.4 and Lemma A.5 therefore yield the existence and uniqueness of the constant b_F and the solution g on \mathbb{R} to the first-order ODE (A.2) such that $xg(x) \leq 0$ for every $x \in \mathbb{R}$. In view of the first-order ODE (A.2) satisfied by g ,

$$g'(x) = \frac{\gamma\sigma^2}{\delta^2}x^2 - F(g(x)) - b_F = \frac{\gamma\sigma^2}{\delta^2}x^2 - \frac{2}{\delta^2}[g(x)(G')^{-1}(g(x)) - G((G')^{-1}(g(x)))] - b_F,$$

Lemma A.6 shows that g is also the unique solution to the ODE (3.5) from Lemma 3.3:

$$\frac{1}{2}\delta^2 g''(x) = -[g(x)(G')^{-1}(g(x)) - G((G')^{-1}(g(x)))]' + \gamma\sigma^2 x = -g'(G')^{-1}(g(x)) + \gamma\sigma^2 x.$$

Here, we have used in the last step that

$$\begin{aligned} & (g(x)(G')^{-1}(g(x)) - G((G')^{-1}(g(x))))' \\ &= g'(x)(G')^{-1}(g(x)) + g(x)((G')^{-1})'(g(x))g'(x) - G'((G')^{-1}(g(x))((G')^{-1})'(g(x))g'(x)) \\ &= g'(x)(G')^{-1}(g(x)) + g(x)((G')^{-1})'(g(x))g'(x) - g(x)((G')^{-1})'(g(x))g'(x) \\ &= g'(x)(G')^{-1}(g(x)). \end{aligned}$$

To complete the proof, notice that

$$F^{-1}(ax^2) = F^{-1}\left(\frac{\gamma\sigma^2}{\delta^2}x^2\right) = (G^*)^{-1}\left(\frac{\delta^2}{2}\frac{\gamma\sigma^2}{\delta^2}x^2\right) = (G^*)^{-1}\left(\frac{\gamma\sigma^2}{2}x^2\right),$$

which yields the analogue of the growth conditions A.6:

$$\lim_{x \rightarrow -\infty} \frac{g(x)}{(G^*)^{-1}\left(\frac{\gamma\sigma^2}{2}x^2\right)} = 1, \quad \lim_{x \rightarrow +\infty} \frac{g(x)}{(G^*)^{-1}\left(\frac{\gamma\sigma^2}{2}x^2\right)} = -1. \quad (\text{A.10})$$

\square

B Calibration Details

In this section, we provide some additional details concerning the calibration of the model with costs of general power form at the end of Section 5.2. If $G_q(x) = \lambda_q|x|^q/q$, $q \in (1, 2]$, then the nonlinear ODE (3.5) from Lemma 3.3 can be simplified by rescaling. Indeed, the solution then can be written as

$$g_q(x) = \left(\frac{\lambda_q}{q}\right)^{\frac{3}{q+2}} \left(\frac{\gamma\sigma^2\delta_q^4}{8}\right)^{\frac{q-1}{q+2}} \tilde{g}_q \left(2^{\frac{q-1}{q+2}} \left(\frac{q\gamma\sigma^2}{\lambda_q}\right)^{\frac{1}{q+2}} \left(\frac{1}{\delta_q}\right)^{\frac{2q}{q+2}} x\right), \quad (\text{B.1})$$

where \tilde{g}_q is the unique solution on \mathbb{R} of⁹

$$\tilde{g}_q''(x) + \tilde{g}_q'(x)\text{sign}(\tilde{g}_q(x)) \left|\frac{\tilde{g}_q(x)}{q}\right|^{\frac{1}{q-1}} = 2x. \quad (\text{B.2})$$

Since this rescaled ODE depends only the elasticity q of the price impact function but not the other model parameters, it only needs to be solved numerically once for each q to match the corresponding parameters λ_q and δ_q the transaction costs and trading volume observed empirically. To wit, the stationary density of the state variable X from Lemma 3.4 is¹⁰

$$\nu_q(x) = c_q \exp\left(-\frac{2}{\delta_q^2} \int_0^x \left|\frac{g_q(y)}{\lambda_q}\right|^{\frac{1}{q-1}} dy\right), \quad \text{where } c_q = \left[2 \int_0^\infty \exp\left(-\frac{2}{\delta_q^2} \int_0^x \left|\frac{g_q(y)}{\lambda_q}\right|^{\frac{1}{q-1}} dy\right) dx\right]^{-1}.$$

We also let v_q denote the variance for ν_q .

The goal now is to choose the model parameters λ_q and δ_q to match the share turnover in the model to its empirical level and the stationary variance of the state variable to its counterpart for proportional costs. To this end, define

$$\tilde{c}_q = \left[2 \int_0^\infty \exp\left(-\int_0^x \left|\frac{\tilde{g}_q(y)}{q}\right|^{\frac{1}{q-1}} dy\right) dx\right]^{-1}, \quad \tilde{v}_q = 2\tilde{c}_q \int_0^\infty x^2 \exp\left(-\int_0^x \left|\frac{\tilde{g}_q(y)}{q}\right|^{\frac{1}{q-1}} dy\right) dx$$

and note that we have

$$c_q = 2^{\frac{q-1}{q+2}} \left(\frac{q\gamma\sigma^2}{\lambda_q}\right)^{\frac{1}{q+2}} \left(\frac{1}{\delta_q}\right)^{\frac{2q}{q+2}} \tilde{c}_q. \quad (\text{B.3})$$

To match the total share turnover, we therefore need

$$\text{ShTu} = \int_{-\infty}^\infty \left|\frac{g_q(x)}{\lambda_q}\right|^{\frac{1}{q-1}} \nu_q(x) dx = c_q \delta_q^2 = 2^{\frac{q-1}{q+2}} \left(\frac{q\gamma\sigma^2}{\lambda_q}\right)^{\frac{1}{q+2}} \left(\frac{1}{\delta_q}\right)^{\frac{2q}{q+2}} \tilde{c}_q \delta_q^2 \quad (\text{B.4})$$

With the same trick here, we can calculate the variance of the stationary law

$$2c_q \int_0^\infty x^2 \nu_q(x) dx = \frac{\tilde{v}_q}{4^{\frac{q-1}{q+2}} \left(\frac{q\gamma\sigma^2}{\lambda_q}\right)^{\frac{2}{q+2}} \left(\frac{1}{\delta_q}\right)^{\frac{4q}{q+2}}}.$$

⁹As shown in Lemma A.6, \tilde{g}_q is in fact the solution to the first-order equation (17) in [27, Theorem 6], with $q = \alpha + 1$.

¹⁰Notice that for quadratic costs $q = 2$, this is the standard normal distribution.

As a result, we can thus match the standard deviation of the stationary law ν_q with the corresponding value $l/\sqrt{3}$ for proportional transaction costs,

$$\frac{l}{\sqrt{3}} = \frac{\sqrt{\tilde{v}_q}}{2^{\frac{q-1}{q+2}} \left(\frac{q\gamma\sigma^2}{\lambda_q}\right)^{\frac{1}{q+2}} \left(\frac{1}{\delta_q}\right)^{\frac{2q}{q+2}}}. \quad (\text{B.5})$$

Conditions (B.4) and (B.5) in turn lead to

$$\delta_q = \left(\frac{(\text{ShTu})^2 l^2}{3\tilde{c}_q^2 \tilde{v}_q}\right)^{\frac{1}{4}} \quad \text{as well as} \quad \lambda_q = \left(\frac{2\tilde{c}_q}{\text{ShTu}}\right)^q \frac{q\gamma\sigma^2 l^2}{6\tilde{v}_q}. \quad (\text{B.6})$$

In summary, for a given value of q , the solution \tilde{g}_q of (B.2) therefore needs to be computed numerically on a fine grid once. Then, we can use numerical integration to approximate \tilde{c}_q , \tilde{v}_q and in turn compute δ_q , λ_q via (B.6).

References

- [1] R. F. Almgren. Optimal execution with nonlinear impact functions and trading-enhanced risk. *Appl. Math. Finance*, 10(1):1–18, 2003.
- [2] R. F. Almgren and N. Chriss. Optimal execution of portfolio transactions. *J. Risk*, 3:5–40, 2001.
- [3] R. F. Almgren and T. M. Li. Option hedging with smooth market impact. *Market Microstructure Liq.*, 2(1), 2016.
- [4] R. F. Almgren, C. Thum, E. Hauptmann, and H. Li. Direct estimation of equity market impact. *RISK*, July, 2005.
- [5] Y. Amihud, H. Mendelson, and L. H. Pedersen. Liquidity and asset prices. *Foundations and Trends in Finance*, 1(4):269–364, 2006.
- [6] S. Ankirchner and T. Kruse. Optimal position targeting with stochastic linear–quadratic costs. *Banach Center Publ.*, 104(1):9–24, 2015.
- [7] P. Bank, H. M. Soner, and M. Voß. Hedging with temporary price impact. *Math. Fin. Econ.*, 11(2):215–239, 2017.
- [8] E. Bayraktar, T. Cayé, and I. Ekren. Asymptotics for small nonlinear price impact: a PDE homogenization approach to the multidimensional case. Preprint, 2018.
- [9] B. Bouchard, M. Fukasawa, M. Herdegen, and J. Muhle-Karbe. Equilibrium returns with transaction costs. *Finance Stoch.*, 22(3):569–601, 2018.
- [10] A. Buss and B. Dumas. The dynamic properties of financial-market equilibrium with trading fees. *J. Finance*, to appear, 2017.
- [11] J. Cai, M. Rosenbaum, and P. Tankov. Asymptotic lower bounds for optimal tracking: a linear programming approach. *Ann. Appl. Probab.*, 27(4):2455–2514, 2017.
- [12] Á. Cartea and S. Jaimungal. A closed-form execution strategy to target volume weighted average price. *SIAM J. Fin. Math.*, 7(1):760–785, 2016.
- [13] T. Cayé, M. Herdegen, and J. Muhle-Karbe. Scaling limits of processes with fast nonlinear mean reversion. Preprint, 2017.
- [14] T. Cayé, M. Herdegen, and J. Muhle-Karbe. Trading with small nonlinear price impact. Preprint, 2018.
- [15] C. Chicone. Ordinary differential equations with applications. *Springer*, 1999.
- [16] J. H. Choi and K. Larsen. Taylor approximation of incomplete Radner equilibrium models. *Finance Stoch.*, 19(3):653–679, 2015.
- [17] J. H. Choi, K. Larsen, and D. J. Seppi. Smart TWAP trading in continuous-time equilibria. Preprint, 2018.
- [18] J. De Lataillade, C. Deremble, M. Potters, and J.-P. Bouchaud. Optimal trading with linear costs. *RISK*, 1(3):2047–1246, 2012.
- [19] B. Dumas and E. Luciano. An exact solution to a dynamic portfolio choice problem under transactions costs. *J. Finance*, 46(2):577–595, 1991.
- [20] I. Ekeland and R. Temam. *Convex analysis and variational problems*. SIAM, Philadelphia, PA, 1999.
- [21] N. Garleanu and L. H. Pedersen. Dynamic trading with predictable returns and transaction costs. *J. Finance*, 68(6):2309–2340, 2013.

- [22] N. Garleanu and L. H. Pedersen. Dynamic portfolio choice with frictions. *J. Econ. Theory*, 165:487–516, 2016.
- [23] S. Gerhold, P. Guasoni, J. Muhle-Karbe, and W. Schachermayer. Transaction costs, trading volume, and the liquidity premium. *Finance Stoch.*, 18(1):1–37, 2014.
- [24] I. Goodfellow, Y. Bengio, and A. Courville. *Deep Learning*. MIT Press, Cambridge, MA, 2016.
- [25] P. Guasoni and M. Rásonyi. Hedging, arbitrage and optimality with superlinear frictions. *Ann. Appl. Probab.*, 25(4):2066–2095, 2015.
- [26] P. Guasoni and M. Weber. Dynamic trading volume. *Math. Finance*, 27(2):313–349, 2017.
- [27] P. Guasoni and M. Weber. Nonlinear price impact and portfolio choice. Preprint, 2018.
- [28] J. Han, A. Jentzen, and W. E. Solving high-dimensional partial differential equations using deep learning. *Proc. Natl. Acad. Sci.*, 115(34):8505–8510, 2018.
- [29] M. Herdegen, J. Muhle-Karbe, and D. Possamai. Equilibrium asset pricing with transaction costs. Preprint, 2019.
- [30] S. Ioffe and C. Szegedy. Batch normalization: Accelerating deep network training by reducing internal covariate shift. In *Proceedings of the 32nd International Conference on Machine Learning*, pages 448–456, 2015.
- [31] K. Janeček and S. E. Shreve. Futures trading with transaction costs. *Illinois J. Math.*, 54(4):1239–1284, 2010.
- [32] J. Kallsen and J. Muhle-Karbe. The general structure of optimal investment and consumption with small transaction costs. *Math. Finance*, 27(3):659–703, 2017.
- [33] C. Kardaras, H. Xing, and G. Žitković. Incomplete stochastic equilibria with exponential utilities: close to Pareto optimality. Preprint, 2015.
- [34] D. P. Kingma and J. Ba. Adam: a method for stochastic optimization. *Proceedings of the International Conference on Learning Representations (ICLR)*, 2015.
- [35] M. Kohlmann and S. Tang. Global adapted solution of one-dimensional backward stochastic Riccati equations, with application to the mean–variance hedging. *Stochastic Process. Appl.*, 97(2):255–288, 2002.
- [36] L. Kruk, J. Lehoczky, K. Ramanan, and S. Shreve. An explicit formula for the skorokhod map on $[0, a]$. *Ann. Probab.*, 35(5):1740–1768, 2007.
- [37] F. Lillo, J. D. Farmer, and R. N. Mantegna. Master curve for price-impact function. *Nature*, 421:129–130, 2003.
- [38] A. W. Lo, H. Mamaysky, and J. Wang. Asset prices and trading volume under fixed transaction costs. *J. Pol. Econ.*, 112(5):1054–1090, 2004.
- [39] A. W. Lynch and S. Tan. Explaining the magnitude of liquidity premia: The roles of return predictability, wealth shocks, and state-dependent transaction costs. *J. Finance*, 66(4):1329–1368, 2011.
- [40] R. Martin. Optimal trading under proportional transaction costs. *RISK*, 27(8):54–59, 2014.
- [41] R. Martin and T. Schöneborn. Mean reversion pays, but costs. *RISK*, 24(2):84–89, 2011.
- [42] L. Moreau, J. Muhle-Karbe, and H. M. Soner. Trading with small price impact. *Math. Finance*, 27(2):350–400, 2017.
- [43] Y. Sannikov and A. Skrzypacz. Dynamic trading: price inertia and front-running. Preprint, 2016.
- [44] H. M. Soner and N. Touzi. Homogenization and asymptotics for small transaction costs. *SIAM J. Control Optim.*, 51(4):2893–2921, 2013.
- [45] M. Taksar, M. J. Klass, and D. Assaf. A diffusion model for optimal portfolio selection in the presence of brokerage fees. *Math. Oper. Res.*, 13(2):277–294, 1988.
- [46] D. Vayanos. Transaction costs and asset prices: a dynamic equilibrium model. *Rev. Fin. Stud.*, 11(1):1–58, 1998.
- [47] D. Vayanos and J.-L. Vila. Equilibrium interest rate and liquidity premium with transaction costs. *Econ. Theory*, 13(3):509–539, 1999.
- [48] A. Y. Veretennikov. On polynomial mixing bounds for stochastic differential equations. *Stoch. Process. Appl.*, 70(1):115–127, 1997.
- [49] K. Weston. Existence of a Radner equilibrium in a model with transaction costs. *Math. Fin. Econ.*, 12(4):517–539, 2018.
- [50] H. Xing and G. Žitković. A class of globally solvable Markovian quadratic BSDE systems and applications. *Ann. Probab.*, 46(1):491–550, 2018.
- [51] G. Žitković. An example of a stochastic equilibrium with incomplete markets. *Finance Stoch.*, 16(2):177–206, 2012.